Spintronics -2

Outline

- Giant Magnetoresistance, Tunneling Magnetoresistance
- Spin Transfer Torque
- Pure Spin current (no net charge current)
 - Spin Hall, Inverse Spin Hall effects
 - Spin Pumping effect
 - Spin Seebeck effect
- Micro and nano Magnetics

Spin polarized current vs pure spin current!

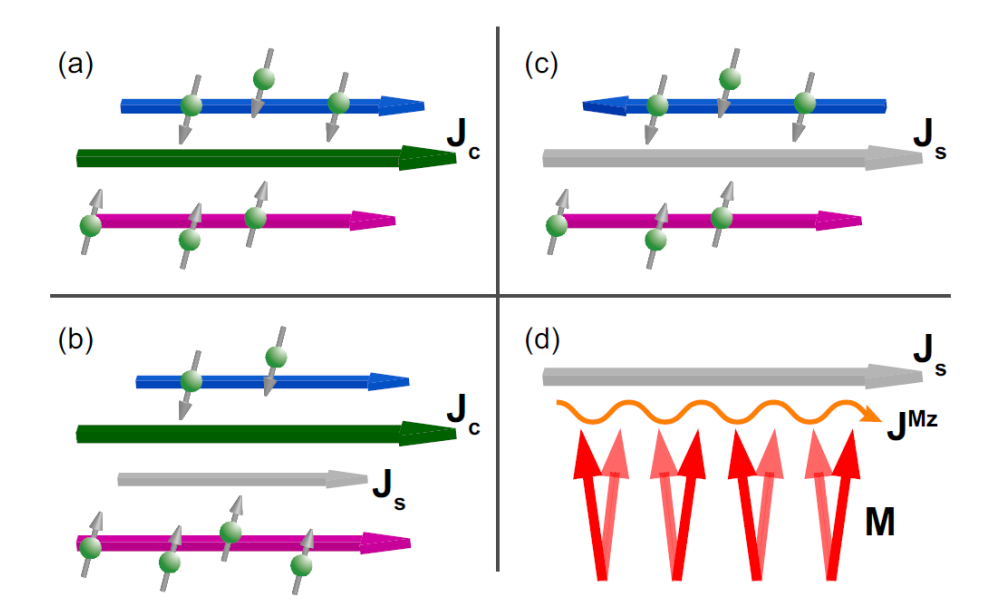
Pure Spin Current

-- with no accompanying net charge current

Theoretically

•
$$J_S = \hat{s} \cdot \vec{v} \rightarrow J_S = \frac{d}{dt} (\hat{s} \cdot \vec{r})$$

- Experimentally
 - Spin Hall, Inverse Spin Hall effects
 - Spin Pumping effect
 - Spin Seebeck effect



Spin Current

Proper Definition of Spin Current in Spin-Orbit Coupled Systems

Junren Shi, 1,2 Ping Zhang, 2,3 Di Xiao, 2 and Qian Niu²

¹Institute of Physics and ICQS, Chinese Academy of Sciences, Beijing 100080, People's Republic of China
 ²Department of Physics, The University of Texas at Austin, Austin, Texas 78712, USA
 ³Institute of Applied Physics and Computational Mathematics, Beijing 100088, People's Republic of China (Received 19 April 2005; revised manuscript received 18 November 2005; published 24 February 2006)

The conventional definition of spin current is incomplete and unphysical in describing spin transport in systems with spin-orbit coupling. A proper and measurable spin current is established in this study, which fits well into the standard framework of near-equilibrium transport theory and has the desirable property to vanish in insulators with localized orbitals. Experimental implications of our theory are discussed.

$$J_S = \hat{s} \cdot \vec{v}$$

$$J_S = \frac{d}{dt}(\hat{s} \cdot \vec{r}) = \hat{s} \cdot \vec{v} + \frac{d}{dt}\hat{s} \cdot \vec{r}$$

torque dipole term

- 1. Spin current is not conserved
- 2. Can even be finite in insulators with localized eigenstates only
- Not in conjugation with any mechanical or thermodynamic force, not fitted into the standard nearequilibrium transport theory

- 1. Spin current conserved
- 2. Vanishes identically in insulators with localized orbitals
- 3. In conjugation with a force given by the gradient of the Zeeman field or spin-dependent chemical potential

Spin Current

Advances in Physics Vol. 59, No. 3, May–June 2010, 181–255



Spin currents and spin superfluidity

E.B. Sonin*

Racah Institute of Physics, Hebrew University of Jerusalem, Jerusalem 91904, Israel (Received 3 September 2009; final version received 1 February 2010)

The present review analyses and compares various types of dissipationless spin transport: (1) Superfluid transport, when the spin-current state is a metastable state (a local but not the absolute minimum in the parameter space). (2) Ballistic spin transport, when spin is transported without losses simply because the sources of dissipation are very weak. (3) Equilibrium spin currents, i.e. genuine persistent currents. (4) Spin currents in the spin Hall effect. Since superfluidity is frequently connected with Bose condensation, recent debates about magnon Bose condensation are also reviewed. For any type of spin currents simplest models were chosen for discussion in order to concentrate on concepts rather than the details of numerous models. The various hurdles on the way of using the concept of spin current (absence of the spin-conservation law, ambiguity of spin current definition, etc.) were analysed. The final conclusion is that the spin-current concept can be developed in a fully consistent manner, and is a useful language for the description of various phenomena in spin dynamics.

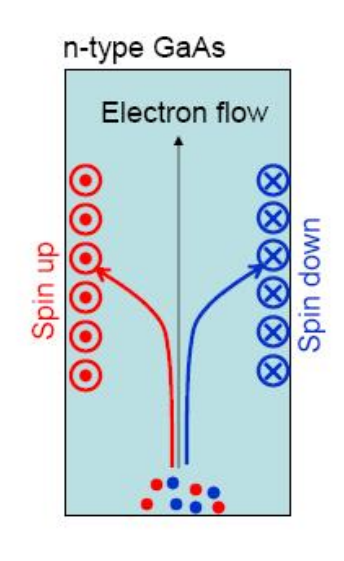
4. Conclusions

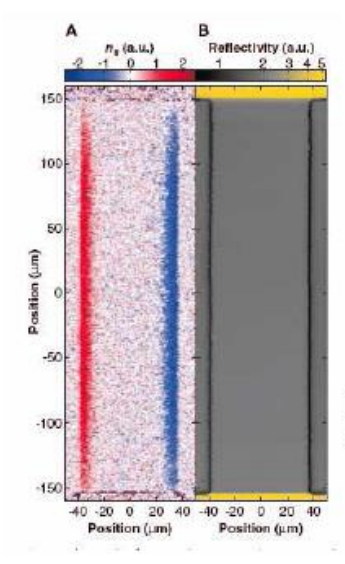
The present review focused on four types of dissipationless spin transport: (1) superfluid transport, when the spin-current state is a metastable state (a local but not the absolute minimum in the parameter space); (2) Ballistic spin transport, when spin is transported without losses simply because the sources of dissipation are very weak; (3) equilibrium spin currents, i.e. genuine persistent currents and (4) spin currents in the spin Hall effect. The dissipationless spin transport was a matter of debate for decades, though sometimes they were to some extent semantic. Therefore, it was important to analyse what physical phenomenon was hidden under this or that name remembering that any choice of terminology is inevitably subjective and is a matter of taste and convention. The various hurdles on the way of using the concept of spin current (absence of the spin-conservation law, ambiguity of spin current definition, etc.) were analysed. The final conclusion is that the spin-current concept can be developed in a fully consistent manner, though this is not an obligatory language of description: spin currents are equivalent to deformations of the spin structure, and one may describe the spin transport also in terms of deformations and spin stiffness.

The recent revival of interest to spin transport is motivated by the emerging of spintronics and high expectations of new applications based on spin manipulation. This is far beyond the scope of the present review, but hopefully the review could justify using of the spin-current language in numerous investigations of spin-dynamics problems, an important example of which is the spin Hall effect.

Spin Hall effect

Spin Hall Effect: Electron flow generates transverse spin current





SHE observed in GaAs using Kerr effect to measure spin M. I. Dyakonov and V. I. Perel, *JETP* **13** 467 (1971)

J. E. Hirsch, Phys. Rev. Lett. 83 1834 (1999)

Guo et al, PRL 100 096401 (2008)

Kato et.al. (Awschalom), Science 306, 1910 (2004)

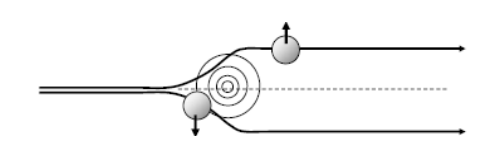
Now observed at room temperature in ZnSe

The Intrinsic SHE is due to topological band structures

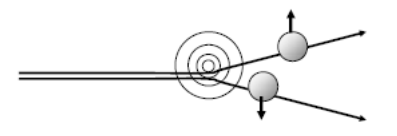
Now observed at room temperature in Zin

Berry curvature
$$\dot{\vec{r}} = \frac{1}{\hbar} \frac{\partial \mathcal{E}_n(\vec{k})}{\partial \vec{k}} + \frac{e}{\hbar} \vec{E} \times \vec{\Omega}(\vec{k})$$

The extrinsic SHE is due to asymmetry in electron scattering for up and down spins. – spin dependent probability difference in the electron trajectories

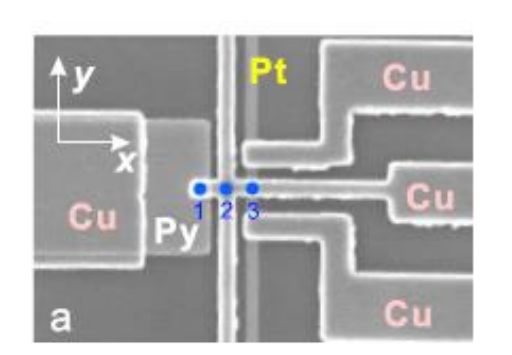


Side jump



Skew scattering

Inverse Spin Hall effect



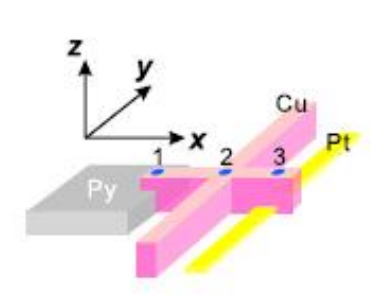
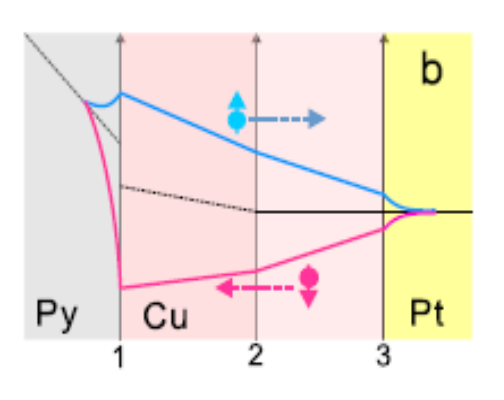
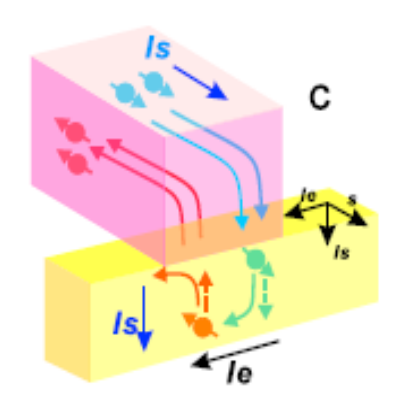
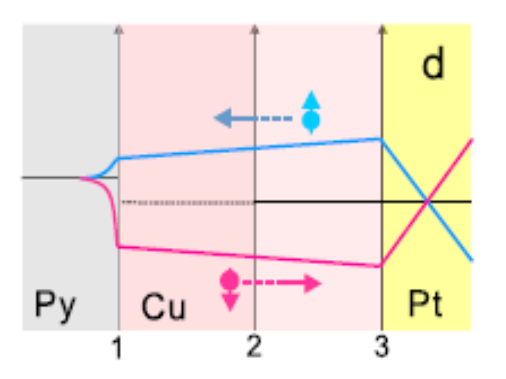
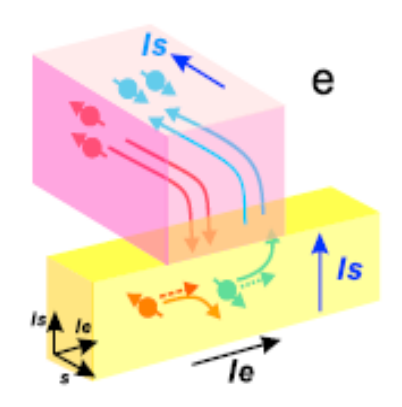


FIG. 1 (color online). (a) Scanning electron microscope (SEM) image of the fabricated spin Hall device together with a schematic illustration of the fabricated device. (b) Schematic spin dependent electrochemical potential map indicating spin accumulation in Cu and Pt induced by the spin injection from the Py pad. Dashed line represents the equilibrium position. (c) Schematic illustration of the charge accumulation process in the Pt wire, where $I_{\rm S}$ and $I_{\rm e}$ denote injected pure spin current and induced charge current, respectively. (d) Spin dependent electrochemical potential map for the charge to spin-current conversion and (e) corresponding schematic illustration.









Kimura et al, PRL 98, 156601 (2007)

Guo et al, PRL 100 096401 (2008)

Inverse Spin Hall effect : ISHE

Volume 83. Number 9

PHYSICAL REVIEW LETTERS

30 August 1999

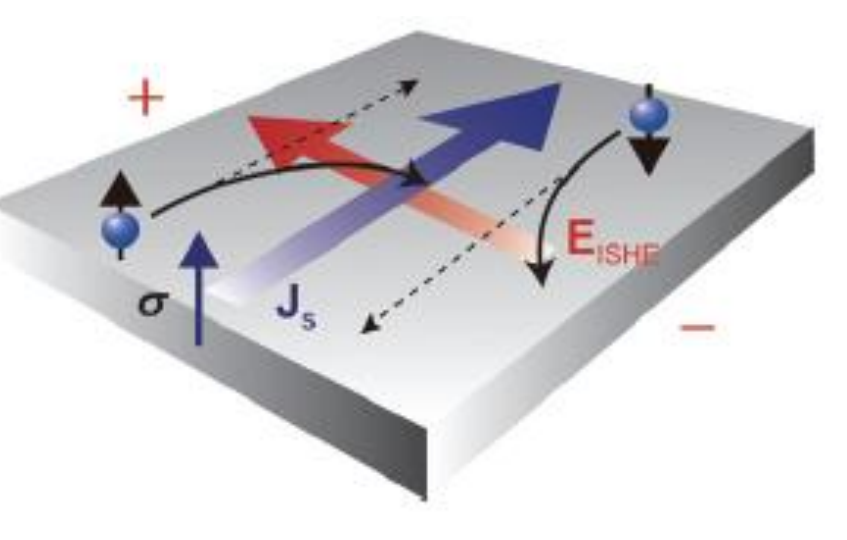
Spin Hall Effect

J. E. Hirsch

Department of Physics, University of California, San Diego, La Jolla, California 92093-0319 (Received 24 February 1999)

It is proposed that when a charge current circulates in a paramagnetic metal a transverse spin imbalance will be generated, giving rise to a "spin Hall voltage." Similarly, it is proposed that when a spin current circulates a transverse charge imbalance will be generated, giving rise to a Hall voltage, in the absence of charge current and magnetic field. Based on these principles we propose an experiment to generate and detect a spin current in a paramagnetic metal.

ISHE: converts a spin current into an electric voltage



J. Appl. Phys. 109, 103913 (2011)

SO-coupling bends the two electrons in the same direction \rightarrow charge accumulation \rightarrow E_{ISHE} .

$$\mathbf{E}_{\mathsf{ISHE}} \propto \mathbf{J}_{\mathit{s}} imes oldsymbol{\sigma}$$

Js: spin current density

σ : direction of the spin-polarization vector of a spin current.

ISHE: Governed by spin-orbit coupling

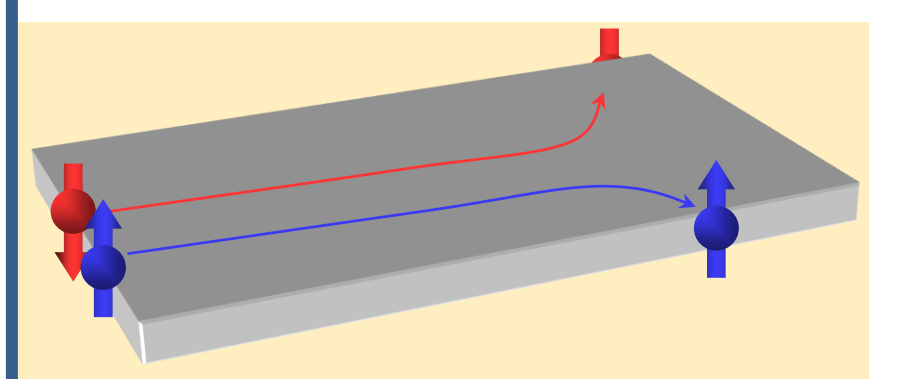
SHE vs ISHE

Spin Hall

Charge Current

Transverse

Spin Imbalance



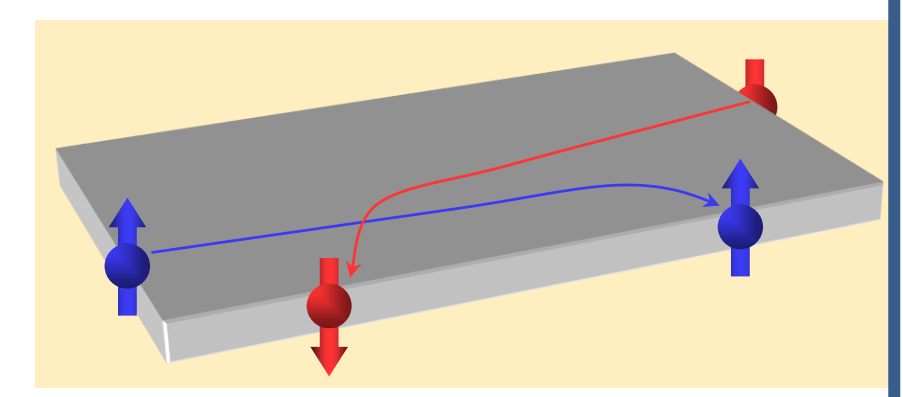
Inverse Spin Hall

Spin Current

J

Transverse

Charge Imbalance



ISHE: direct & sensitive detection of a spin current!

Spin Hall Angle

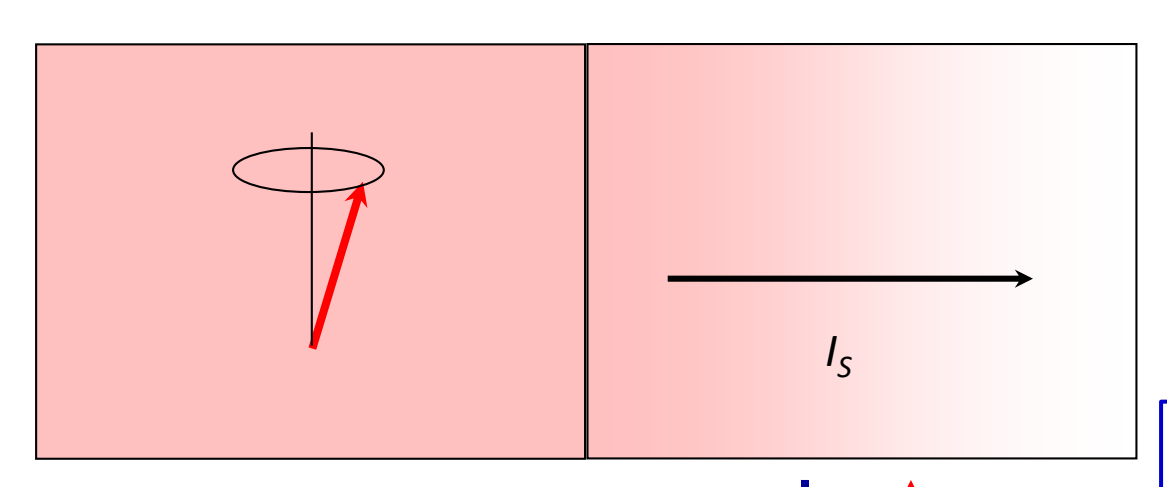
$$\gamma = \frac{\sigma_{SH}}{\sigma_c} \leftarrow \text{spin Hall conductivity}$$

$$\leftarrow \text{charge conductivity}$$

stronger spin orbit interaction \longrightarrow larger γ

Spin Pumping

F N



$$\dot{\mathbf{m}} = -\gamma \mathbf{m} \times \mathbf{H}_{\text{eff}} + \mathbf{m} \times (\tilde{\alpha} \dot{\mathbf{m}})$$

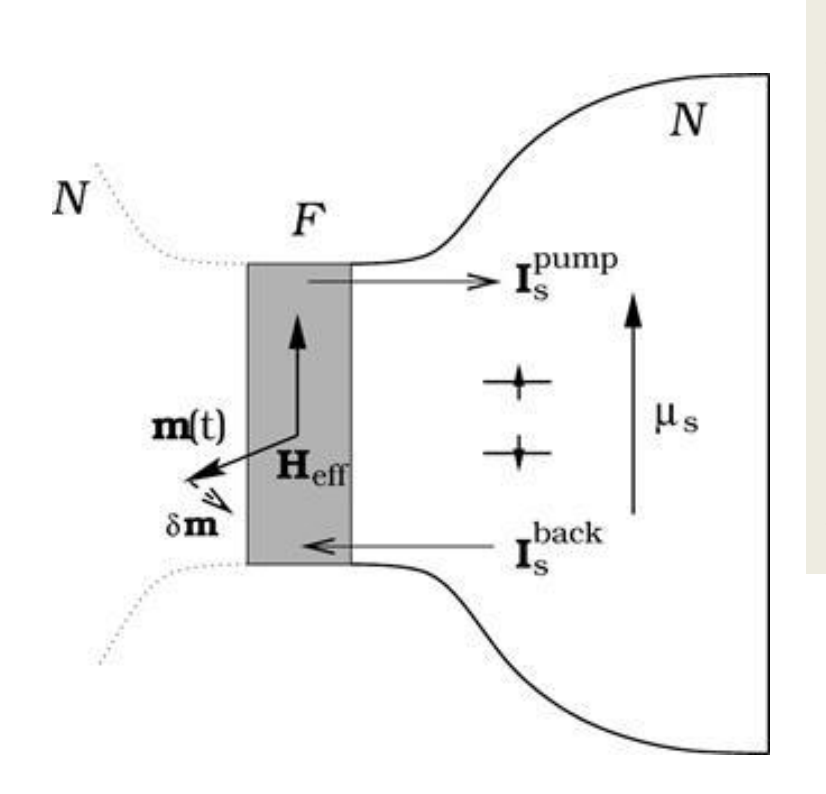
 $I_S^{pump} = \frac{\hbar}{4\pi} g_r^{\downarrow\uparrow} m \times \frac{\partial m}{\partial t}$

 $g_r^{\downarrow\uparrow}$: spin mixing conductance

Spin accumulation gives rise to spin current in neighboring normal metal

In the FMR condition, the steady magnetization precession in a F is maintained by balancing the absorption of the applied microwave and the dissipation of the spin angular momentum --the transfer of angular momentum from the local spins to conduction electrons, which polarizes the conduction-electron spins.

Spin Pumping



A ferromagnetic film F sandwiched between two nonmagnetic reservoirs N. For simplicity of the discussion in this section, we mainly focus on the dynamics in one (right) reservoir while suppressing the other (left), e.g., assuming it is insulating. The spin-pumping current \mathbf{I}_s and the spin accumulation μ_s in the right reservoir can be found by conservation of energy, angular momentum, and by applying circuit theory to the steady state \mathbf{I}_s pump = \mathbf{I}_s back.

$$\mathbf{I}_{s}^{\text{pump}} = \frac{\hbar}{4\pi} \left(A_{r} \mathbf{m} \times \frac{d\mathbf{m}}{dt} - A_{i} \frac{d\mathbf{m}}{dt} \right).$$

- Tserkovnyak et al, PRL 88, 117601 (2002), Enhanced Gilbert Damping in Thin Ferromagnetic Films
- Brataas et al, PRB 66, 060404(R) (2002), Spin battery operated by ferromagnetic resonance
- Tserkovnyak et al, PRB 66, 224403 (2002), Spin pumping and magnetization dynamics in metallic multilayers
- Rev Mod Phys 77, 1375 (2005) Nonlocal magnetization dynamics in ferromagnetic heterostructures

Spin Backflow and ac Voltage Generation by Spin Pumping and the Inverse Spin Hall Effect,

Jiao and Bauer, PRL 110, 217602 (2013)

--- The spin current pumped by a precessing ferromagnet into an adjacent normal metal has a constant polarization component parallel to the precession axis and a rotating one normal to the magnetization. The former is now routinely detected as a dc voltage induced by the inverse spin Hall effect (ISHE). Here we compute ac ISHE voltages much larger than the dc signals for various material combinations, and discuss optimal conditions to observe the effect. The **backflow of spin** is shown to be essential to distill parameters from measured ISHE voltages for both dc and ac configurations.

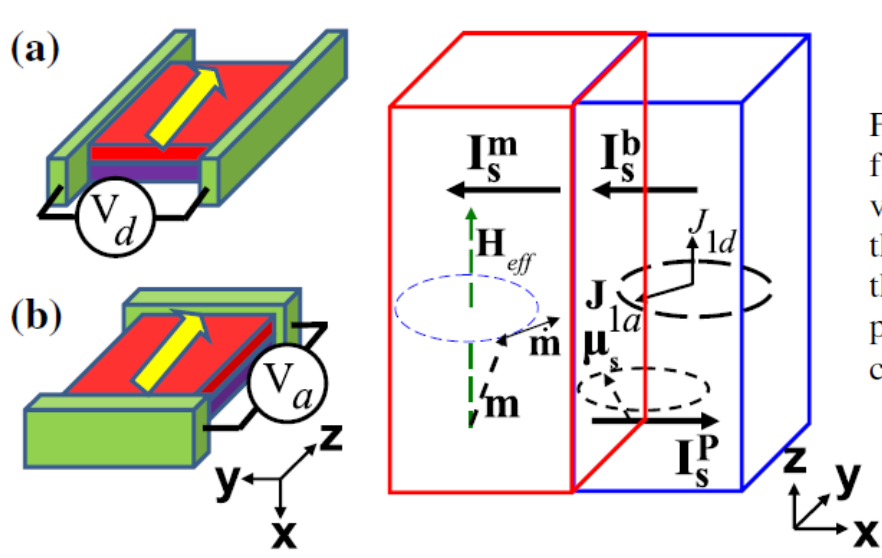
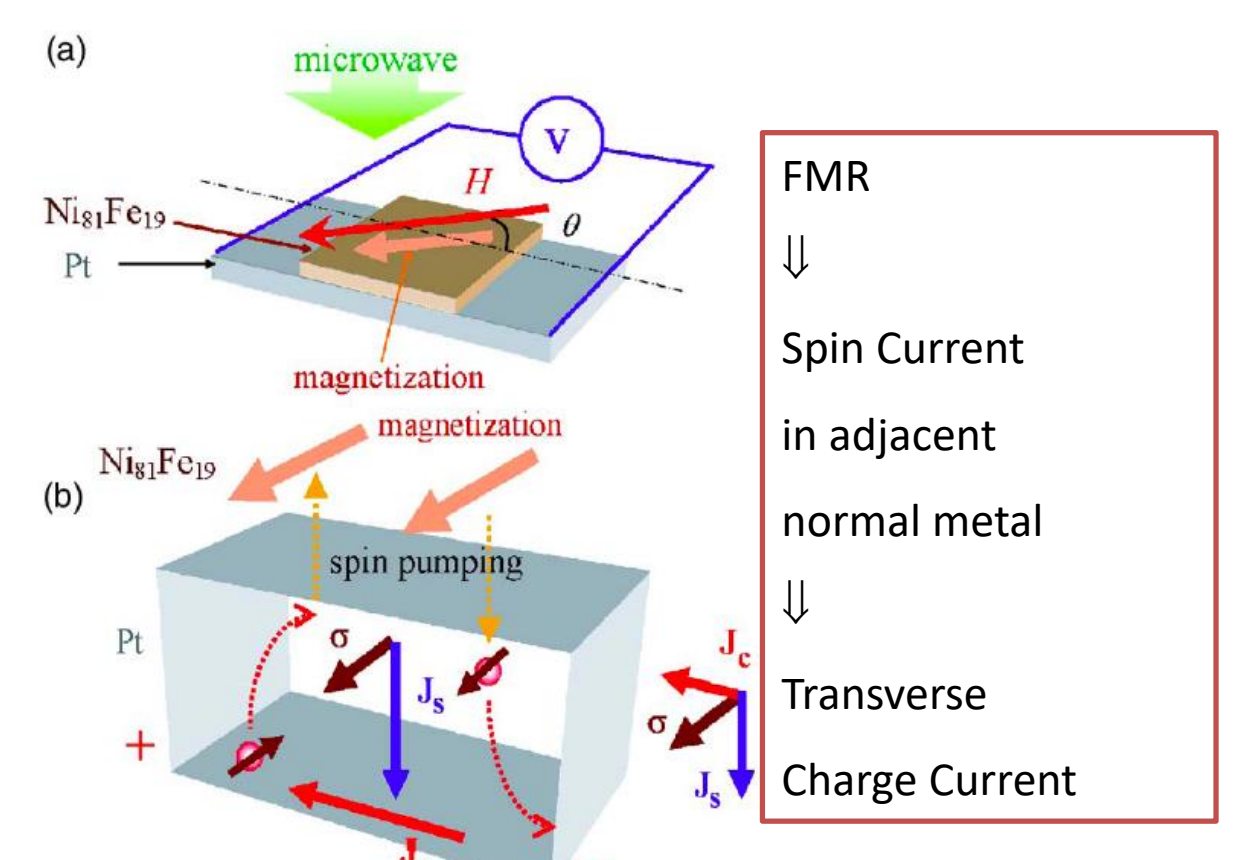


FIG. 1 (color online). Schematic spin battery operated by FMR, for the measurement configurations (a) and (b). The ac (dc) voltage drops along the z(y) direction. The right panel introduces the parameters of the model. The effective field \mathbf{H}_{eff} is the sum of the external field \mathbf{H}_{ex} and the uniaxial field \mathbf{H}_{un} , \mathbf{H}_{ex} , and \mathbf{H}_{un} point along the z axis. The dc component $J_{1d}(j_{1s}^z)\mathbf{e}_z$ and ac component $\mathbf{J}_{1a}(\mathbf{j}_{1s}^a)$ constitute the spin current \mathbf{j}_{1s} .

Combining Spin Pumping and Inverse Spin Hall Effect



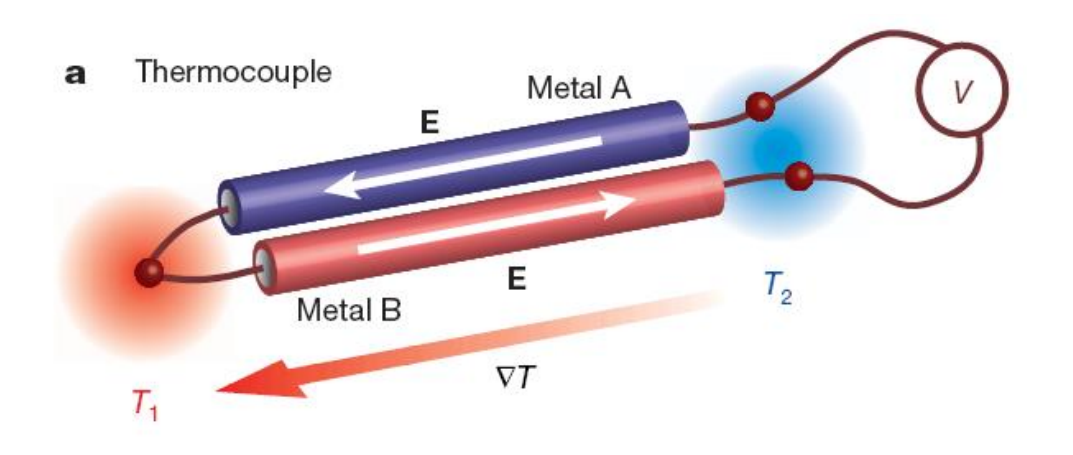
The spin-orbit interaction bends these two electrons in the same direction and induces a charge current transverse to Js,

$$J_c = D_{ISHE}J_s \times \sigma$$
.

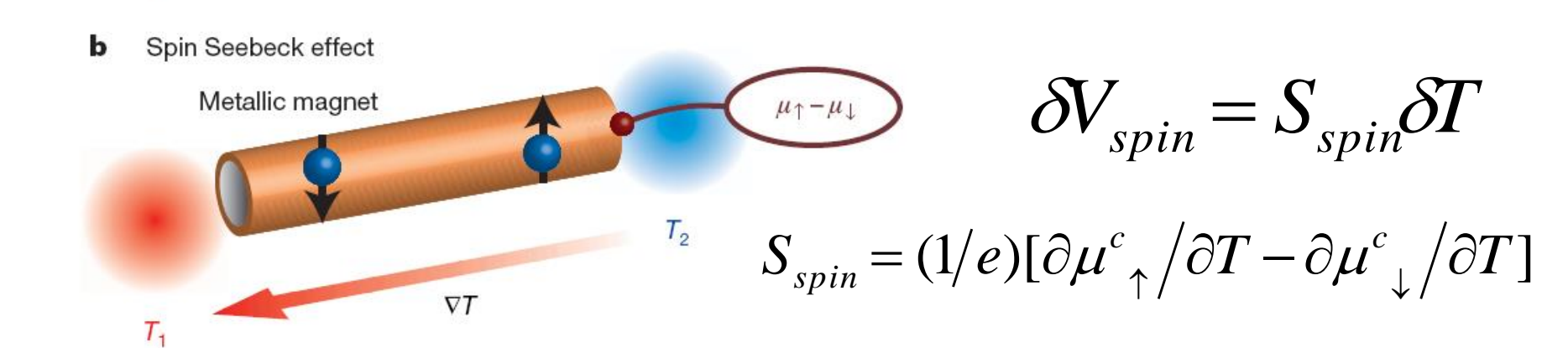
The surface of the Py layer is of a 1×1 mm² square shape. Two electrodes are attached to both ends of the Pt layer.

Saitoh *et al*, APL **88**, 182509 (2006) Kimura *et al*, PRL **98**, 156601 (2007)

Spin Seebeck effect



$$\delta V = S \delta T$$

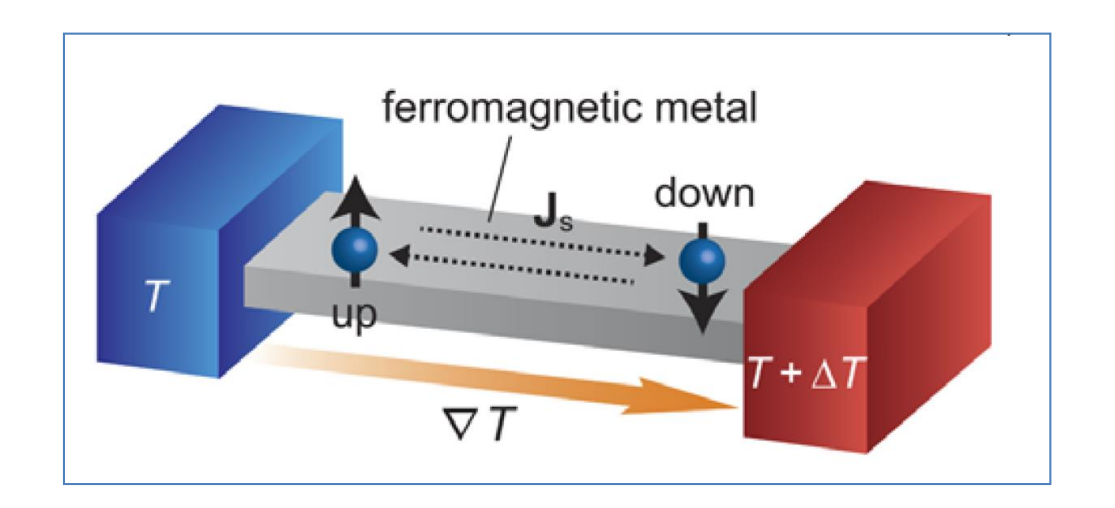


Spin Seebeck effect

In a ferromagnetic metal, **up-spin and down-spin conduction** electrons have **different scattering rates and densities**, and thus have different Seebeck coefficients.

$$\boldsymbol{j}_{s} = \boldsymbol{j}_{\uparrow} - \boldsymbol{j}_{\downarrow} = (\boldsymbol{\sigma}_{\uparrow} \boldsymbol{S}_{\uparrow} - \boldsymbol{\sigma}_{\downarrow} \boldsymbol{S}_{\downarrow})(-\nabla \boldsymbol{T})$$

This **Spin current** flows without accompanying charge currents in the open-circuit condition, and the up-spin and down-spin currents flow in opposite directions along the temperature gradient

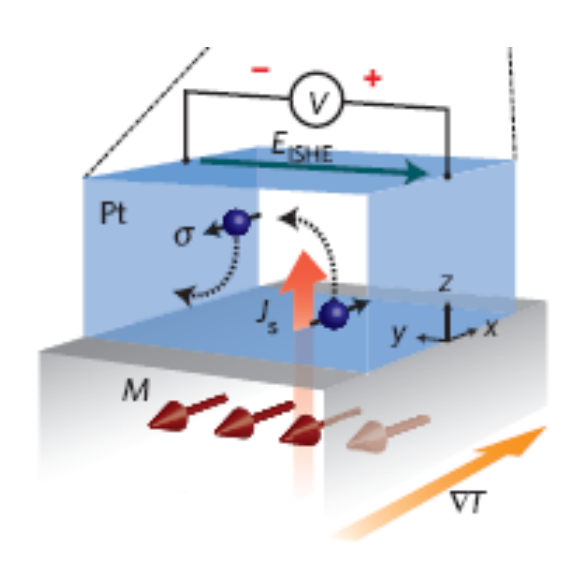


How to detect j_s ?

Inverse Spin Hall Effect coverts j_s into j_c

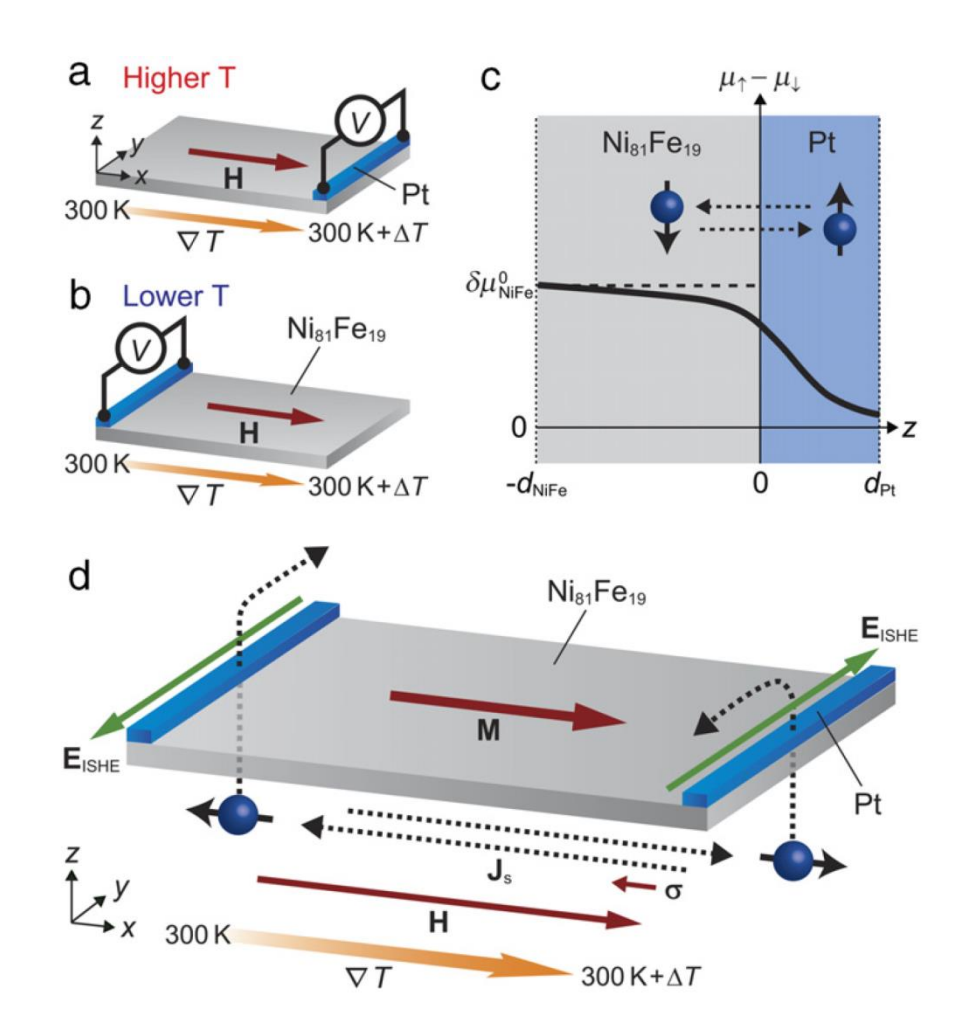
Detection of Spin Current by Inverse Spin Hall Effect

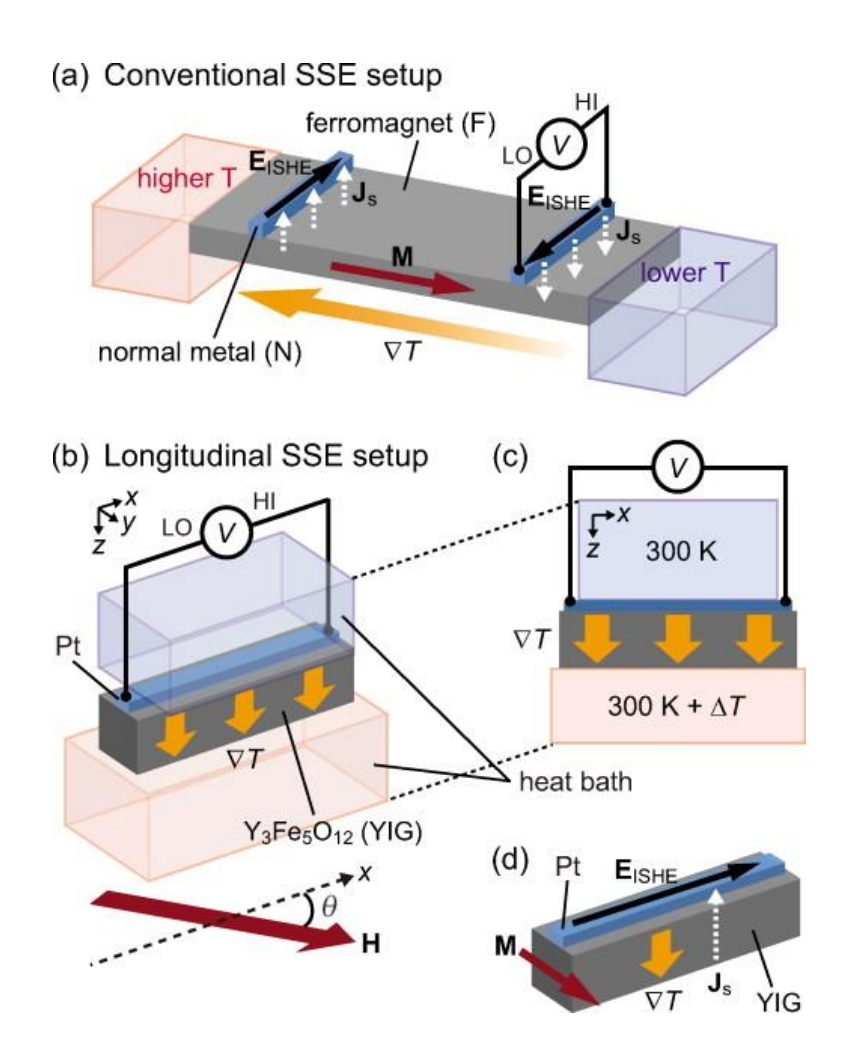
The ISHE converts a spin current into an electromotive force E_{SHE} by means of spin-orbit scattering.



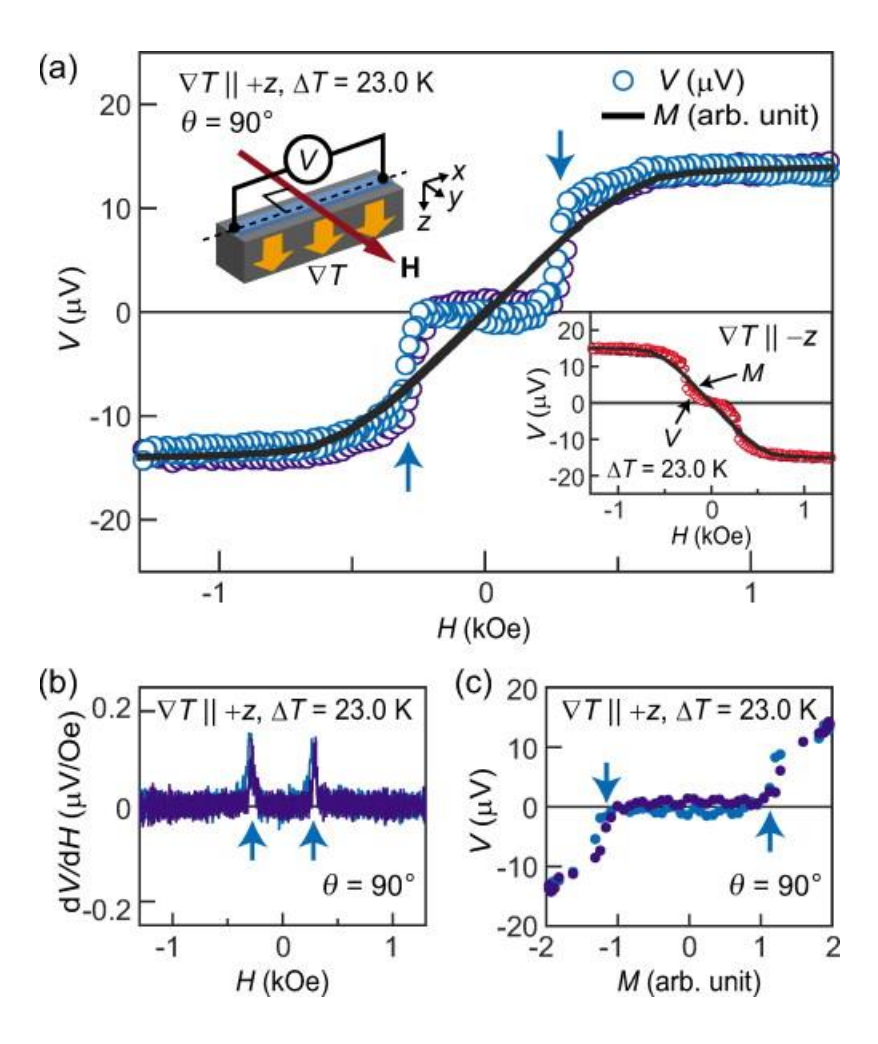
$$E_{y} = E_{SHE} = D_{ISHE} J_{S} \times \sigma$$

A spin current carries a spin-polarization vector σ along a spatial direction J_s .





(a) A schematic of the conventional setup for measuring the ISHE induced by the SSE. Here, ∇T, M, Js, and EISHE denote a temperature gradient, the magnetization vector of a ferromagnet (F), the spatial direction of the spin current flowing across the F/no...



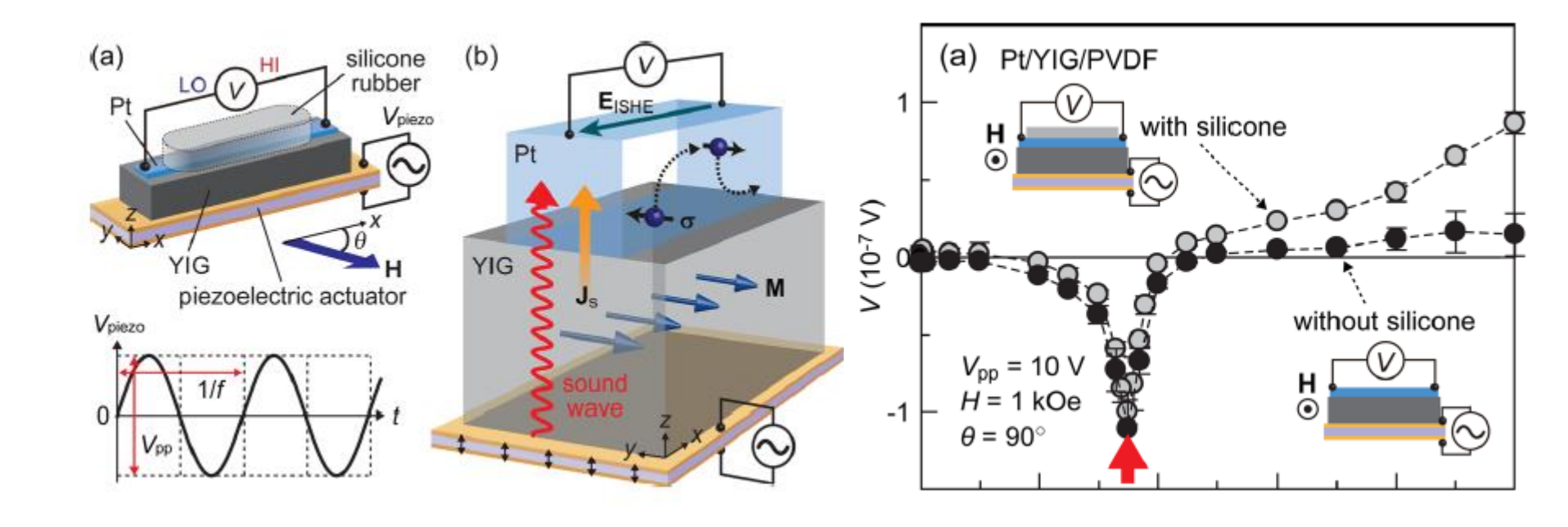
(a) Comparison between the H dependence of V at $\Delta T = 23.0$ K in the YIG/Pt system and the magnetization M curve of the YIG. During the V measurements, ∇T was applied along the +z direction [the -z direction for the inset to (a)] and H was applied along the...

Sound waves

JOURNAL OF APPLIED PHYSICS 111, 053903 (2012)

Acoustic spin pumping: Direct generation of spin currents from sound waves in Pt/Y₃Fe₅O₁₂ hybrid structures

K. Uchida, $^{1,2,a)}$ H. Adachi, 2,3 T. An, 1,2 H. Nakayama, 1,2 M. Toda, 4 B. Hillebrands, 5 S. Maekawa, 2,3 and E. Saitoh 1,2,3

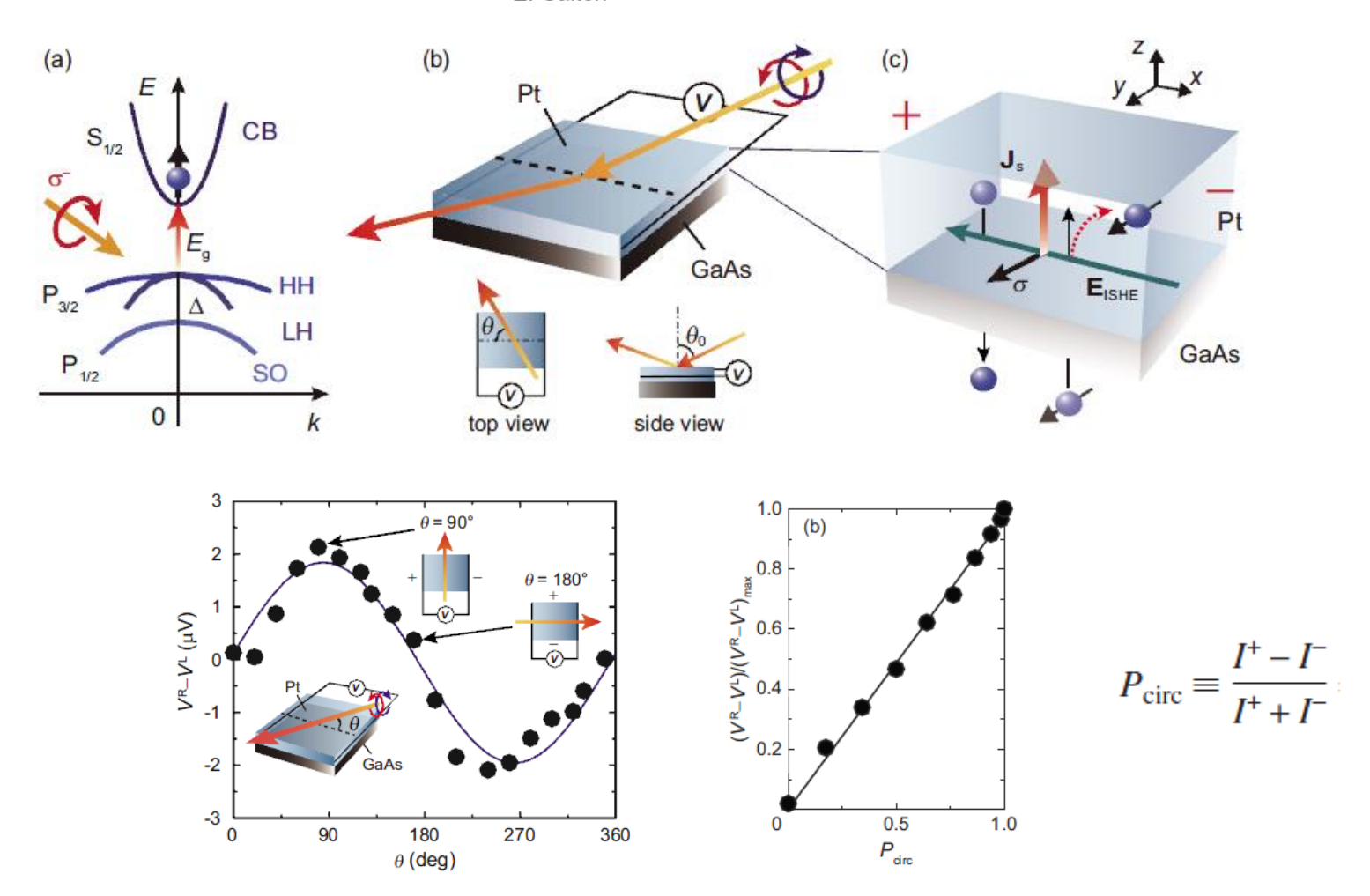


Circularly polarized light

APPLIED PHYSICS LETTERS 96, 082502 (2010)

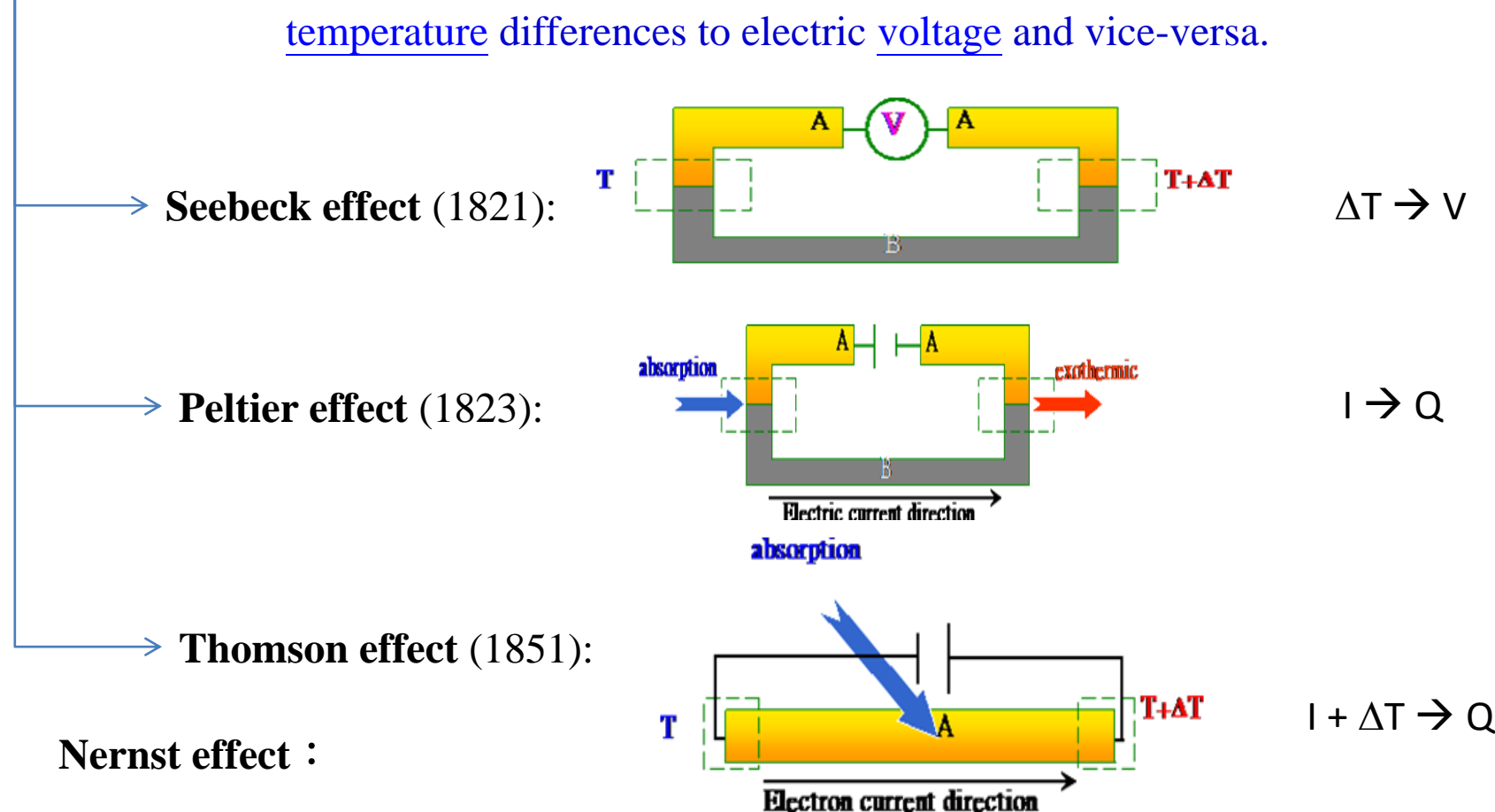
Photoinduced inverse spin-Hall effect: Conversion of light-polarization information into electric voltage

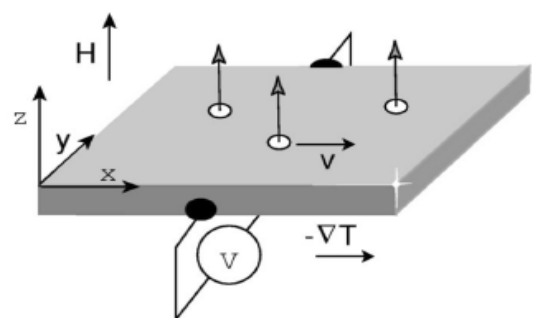
K. Ando, ^{1,2,a)} M. Morikawa, ² T. Trypiniotis, ³ Y. Fujikawa, ¹ C. H. W. Barnes, ³ and E. Saitoh ^{1,2,4}



Thermoelectric effect:

The thermoelectric effect is the direct conversion of



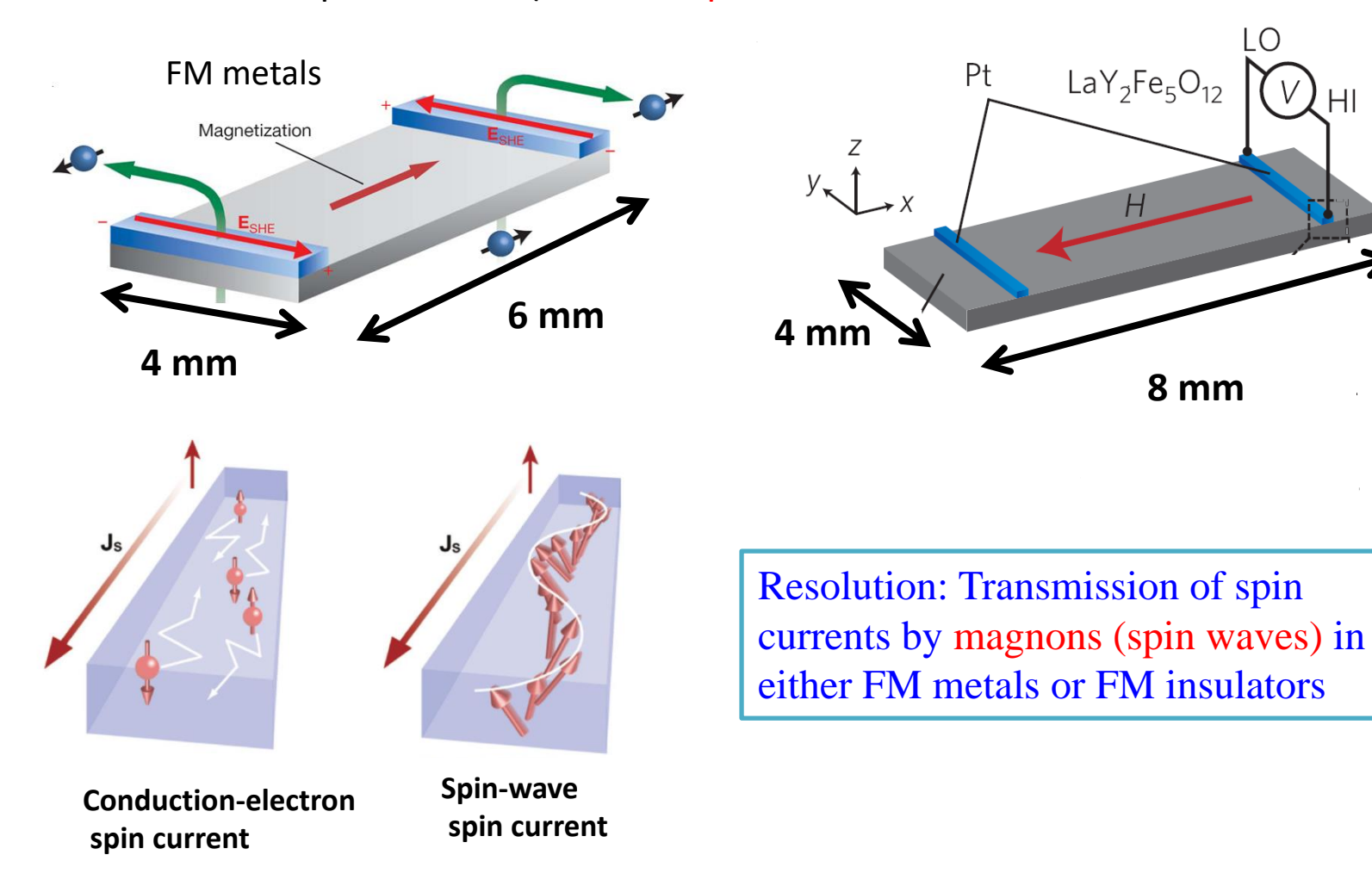


When a sample is subjected to a magnetic field and a temperature gradient normal (perpendicular) to each other, an electric field will be induced normal to both.

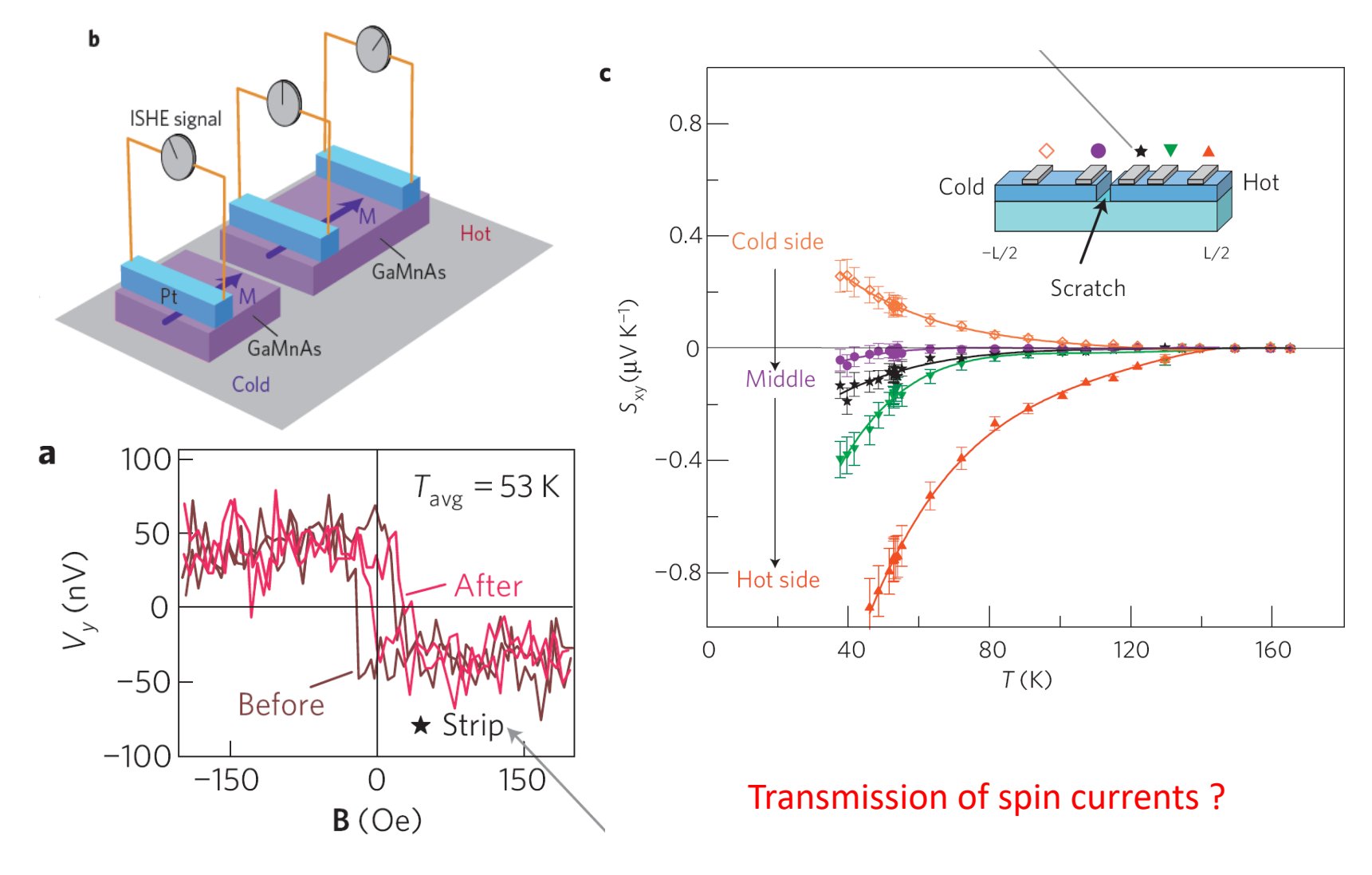
Mystery 1:

Transmission of Spin Current in Metal and Insulator

Over macroscopic distance (mm's >> spin diffusion length) without dissipation?

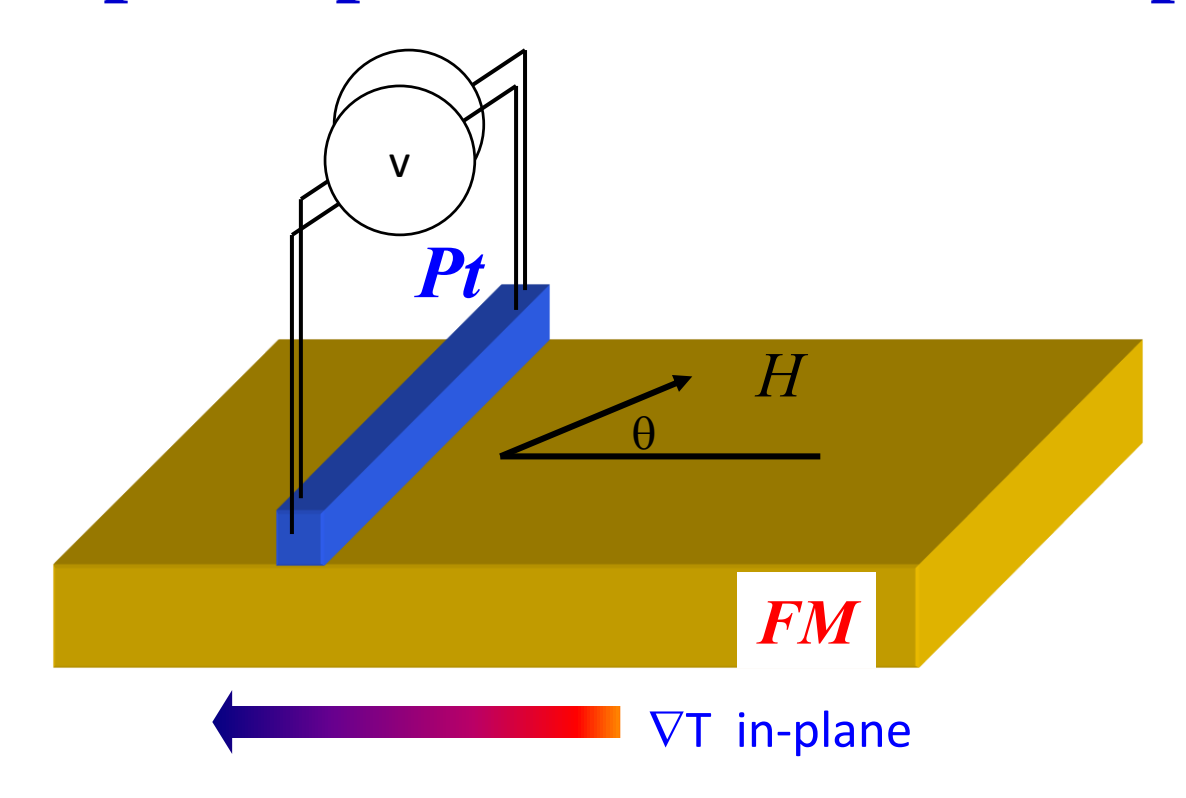


Mystery 2: Spin Seebeck effect in broken FM semiconductor



Intrinsic Caloritronic effects (not substrate dominated) ?

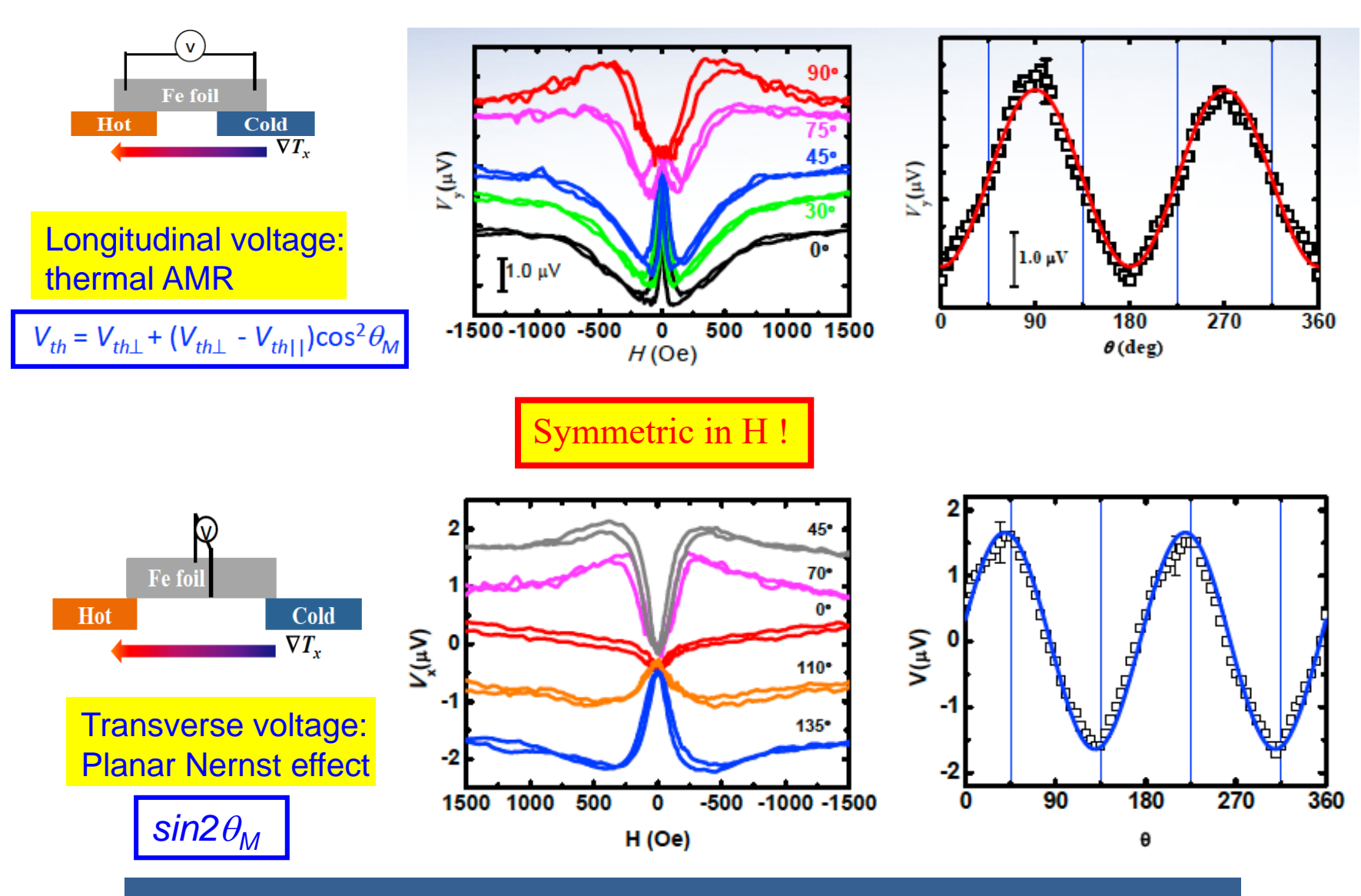
Intrinsic spin Seebeck effect? Intrinsic spin-dependent thermal transport?



Huang, Wang, Lee, Kwo, and CLC,

"Intrinsic spin-dependent thermal transport," PRL 107, 216604 (2011)

Intrinsic spin caloritronic properties with in-plane $\nabla_{x}T$



Necessary Signatures of FM film with in-plane $\nabla_{x}T$

1. Thin film/substrate, in-plane $(\nabla_{r}T)$ and perpendicular $(\nabla_{r}T)$

Spin Seebeck effect $(\nabla_{\mathbf{r}} T)$ with Pt

Anomalous Nernst effect $(\nabla_{\tau}T)$ with or without Pt

2. V_{ANE} and $(V_{\text{SSE}})_{\text{Pt}}$ are additive

If V_{ANE} unknown, $(V_{\text{SSE}})_{\text{Pt}}$ uncertain

Intrinsic spin Seebeck effect?

- 3. ANE: excellent detector of $\nabla_z T$ and ΔT_z
- 4. Intrinsic spin caloritronics with in-plane $\nabla_x T$ in Fe foils Thermal AMR $(cos^2\theta)$ Planar Nernst $(sin 2\theta)$

Necessary conditions for in-plane $\nabla_x T$ only!

Topological insulators



- Topological insulator is a material conducting on its boundary but behaves as an insulator in its bulk.
- The conducting channel(s) are guaranteed by time-reversal symmetry, topologically protected, will not be affected by local impurities etc, and thus robust.

Why the word 'topological'?

 Topological order: a pattern of long-range quantum entanglement in quantum states, can be described by a new set of quantum numbers, such as ground state degeneracy, quasiparticle fractional statistics, edge states, topological entropy, etc.

 Landau symmetry breaking

describes classical orders in materials.

But it failed to describe the chiral spin state, which was proposed (but failed) to explain HTS.

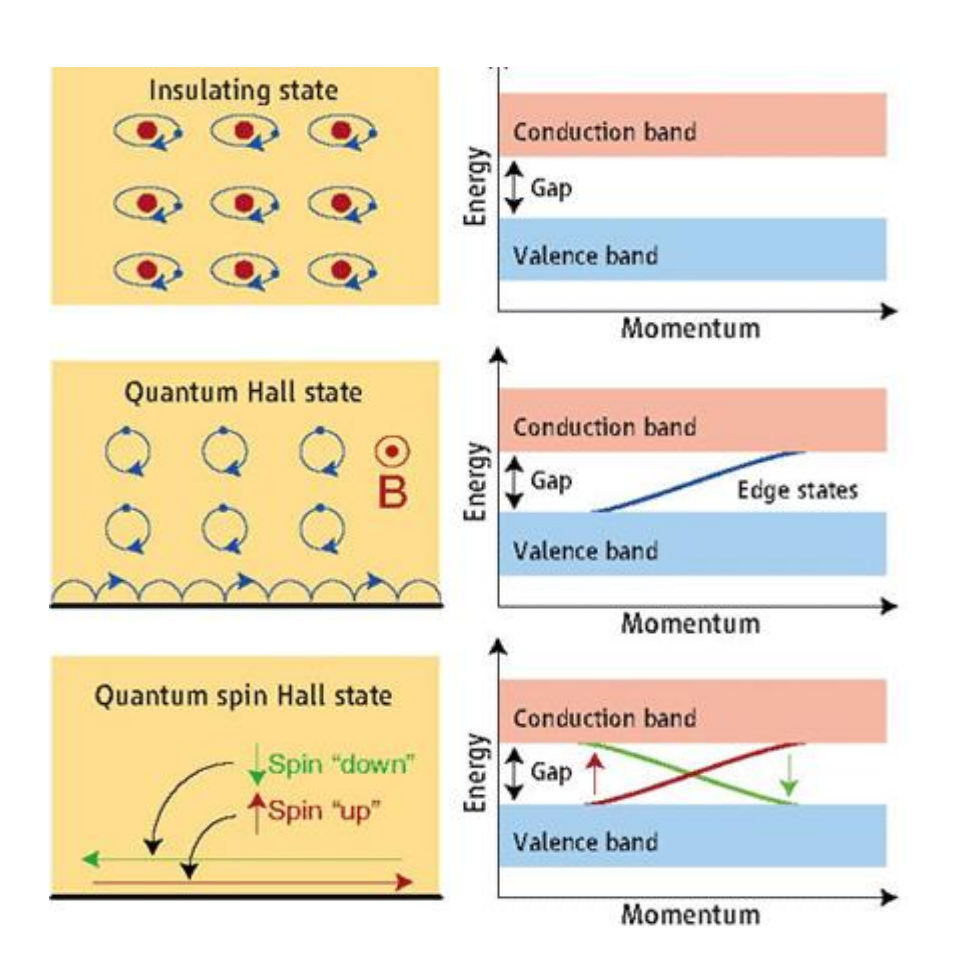
- Z₂ topological quantum number
- Chern numbers (陳省身) explains Quantum Hall Effect (from Foucault pendulum to Chern numbers)

$$1/2\pi \int_{S} K dA = 2 (1 - g)$$

How to become a topological insulator? Or, how to cross from an intrinsic insulator to a topological insulator? Or, how to build the edge conducting states?

- Spin-orbit effect
- Lattice constant adjustment
- To get inversion states and Dirac cone on the boundary.

 Carriers in these states have their spin locked at a right-angle to their momentum.
 At a given energy the only other available electronic states have opposite spin, so scattering is strongly suppressed, and conduction on the surface is nearly dissipationless.



States of matter:

(**Top**) Electrons in an insulator are bound in localized orbitals (left) and have an energy gap (right) separating the occupied valence band from the empty conduction band.

(Middle) A two-dimensional quantum Hall state in a strong magnetic field has a bulk energy gap like an insulator, but permits electrical conduction in one-dimensional "one way" edge states along the sample boundary.

(**Bottom**) The quantum spin Hall state at zero magnetic field also has a bulk energy gap but allows conduction in spin-filtered edge states.

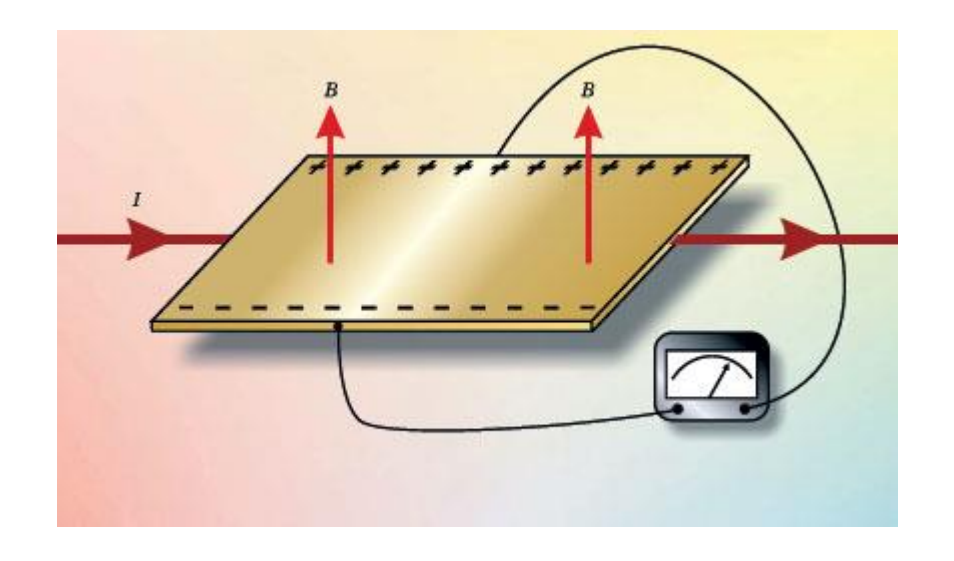
A zoo of Hall effects

• Hall effect --- $B \perp I, V \perp I$

- $R_H = \frac{-n\mu_e^2 + p\mu_h^2}{e(n\mu_e + p\mu_h)^2}$
- Anomalous (Extra-ordinary) Hall effect --extra voltage proportional to magnetization
- Planar Hall effect --- in-plane field, $V \perp I$
- (Integer) Quantum Hall effect --- $B \perp I$, $V \perp I$ in 2D electron gas

 $\sigma = \nu \; \frac{e^2}{h},$

- Fractional Quantum Hall effect --- electrons bind magnetic flux lines
- Spin Hall effect --- $B = 0, V \perp I$
- Quantum Spin Hall effect --- 2D topological insulator



Edwin Hall's 1878 experiment was the first demonstration of the Hall effect. A magnetic field *B* normal to a gold leaf exerts a Lorentz force on a current *I* flowing longitudinally along the leaf. That force separates charges and builds up a transverse "Hall voltage" between the conductor's lateral edges. Hall detected this transverse voltage with a voltmeter that spanned the conductor's two edges.

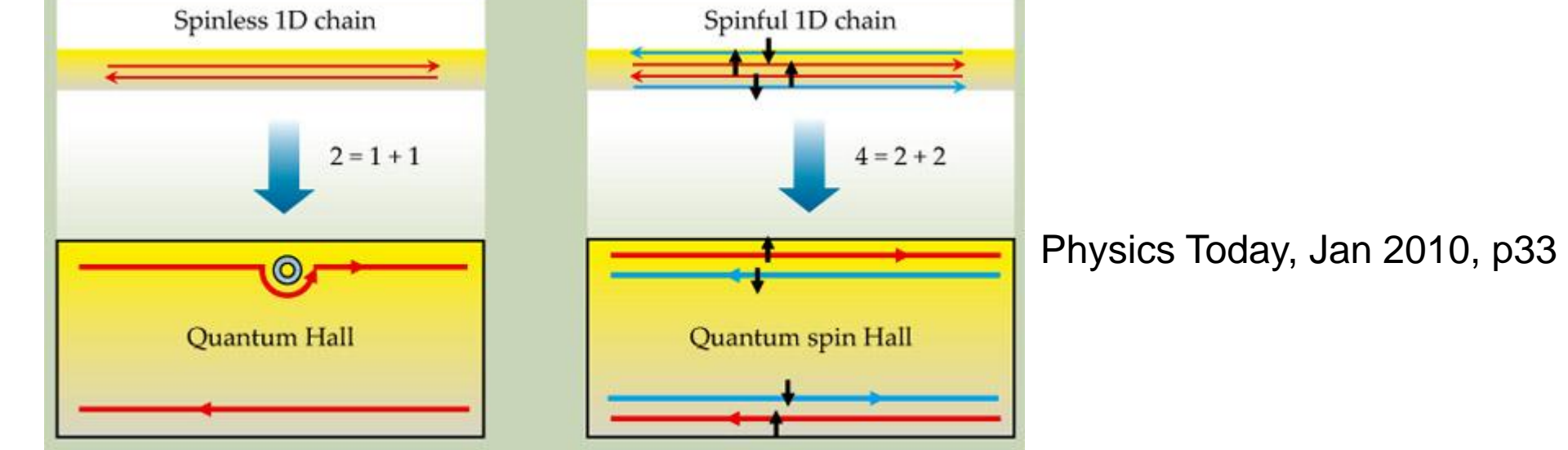


Figure 1. Spatial separation is at the heart of both the quantum Hall (QH) and the quantum spin Hall (QSH) effects. **(a)** A spinless one-dimensional system has both a forward and a backward mover. Those two basic degrees of freedom are spatially separated in a QH bar, as illustrated by the symbolic equation "2 = 1 + 1." The upper edge contains only a forward mover and the lower edge has only a backward mover. The states are robust: They will go around an impurity without scattering. **(b)** A spinful 1D system has four basic channels, which are spatially separated in a QSH bar: The upper edge contains a forward mover with up spin and a backward mover with down spin, and conversely for the lower edge. That separation is illustrated by the symbolic equation "4 = 2 + 2."

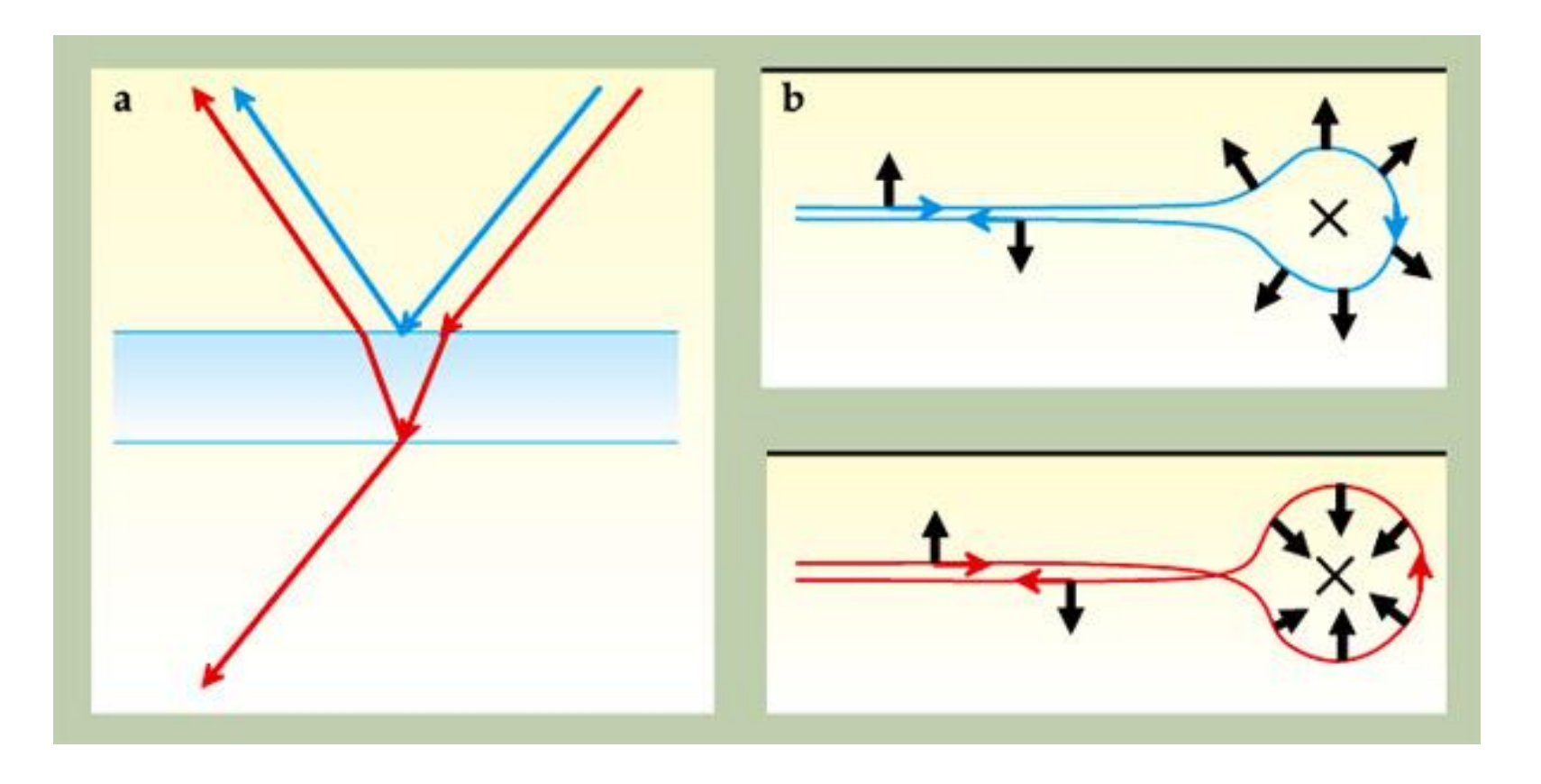


Figure 2. (a) On a lens with antireflection coating, light waves reflected by the top (blue line) and the bottom (red line) surfaces interfere destructively, which leads to suppressed reflection. (b)A quantum spin Hall edge state can be scattered in two directions by a nonmagnetic impurity. Going clockwise along the blue curve, the spin rotates by π ; counterclockwise along the red curve, by $-\pi$. A quantum mechanical phase factor of -1 associated with that difference of 2π leads to destructive interference of the two paths—the backscattering of electrons is suppressed in a way similar to that of photons off the antireflection coating.

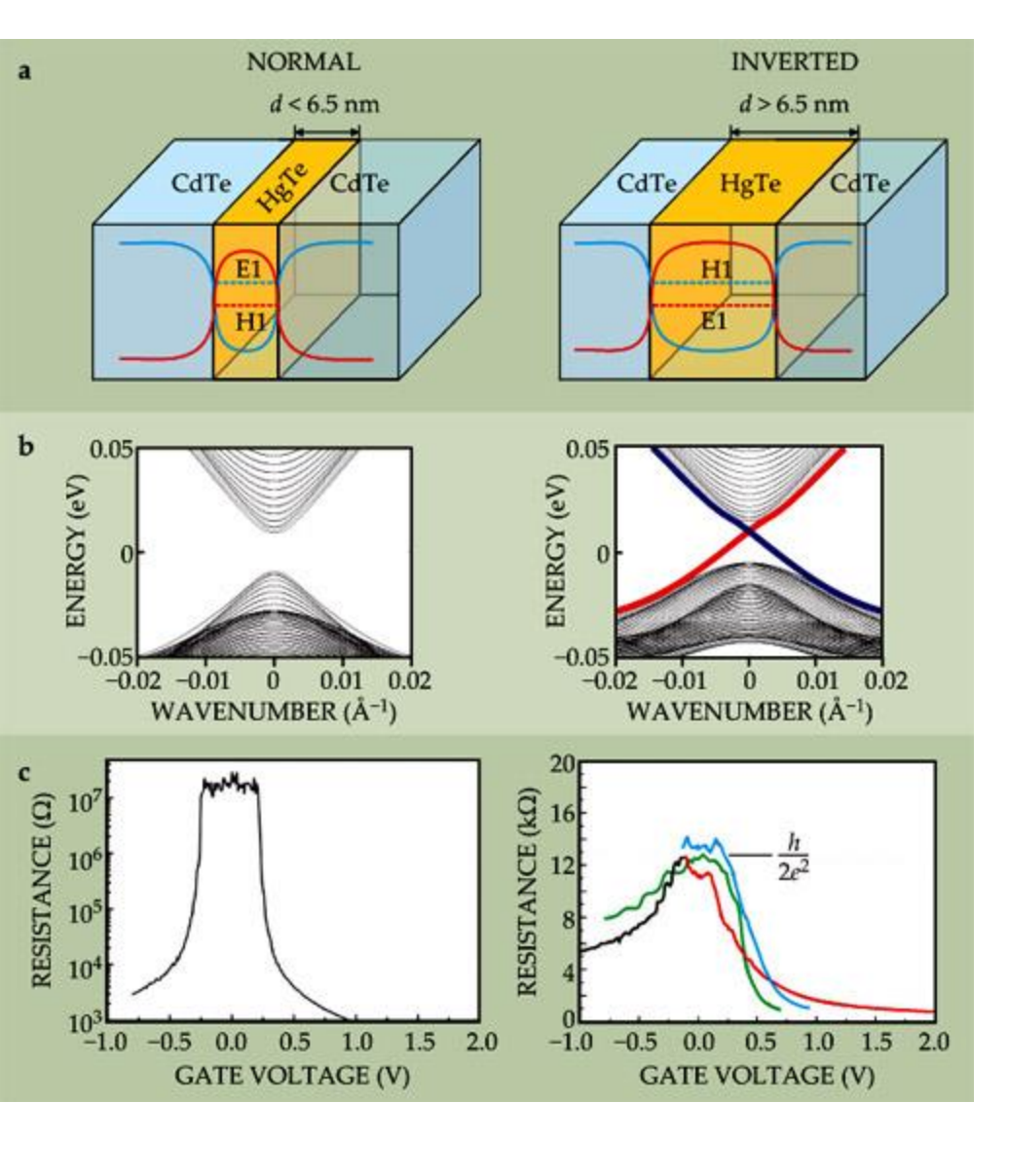


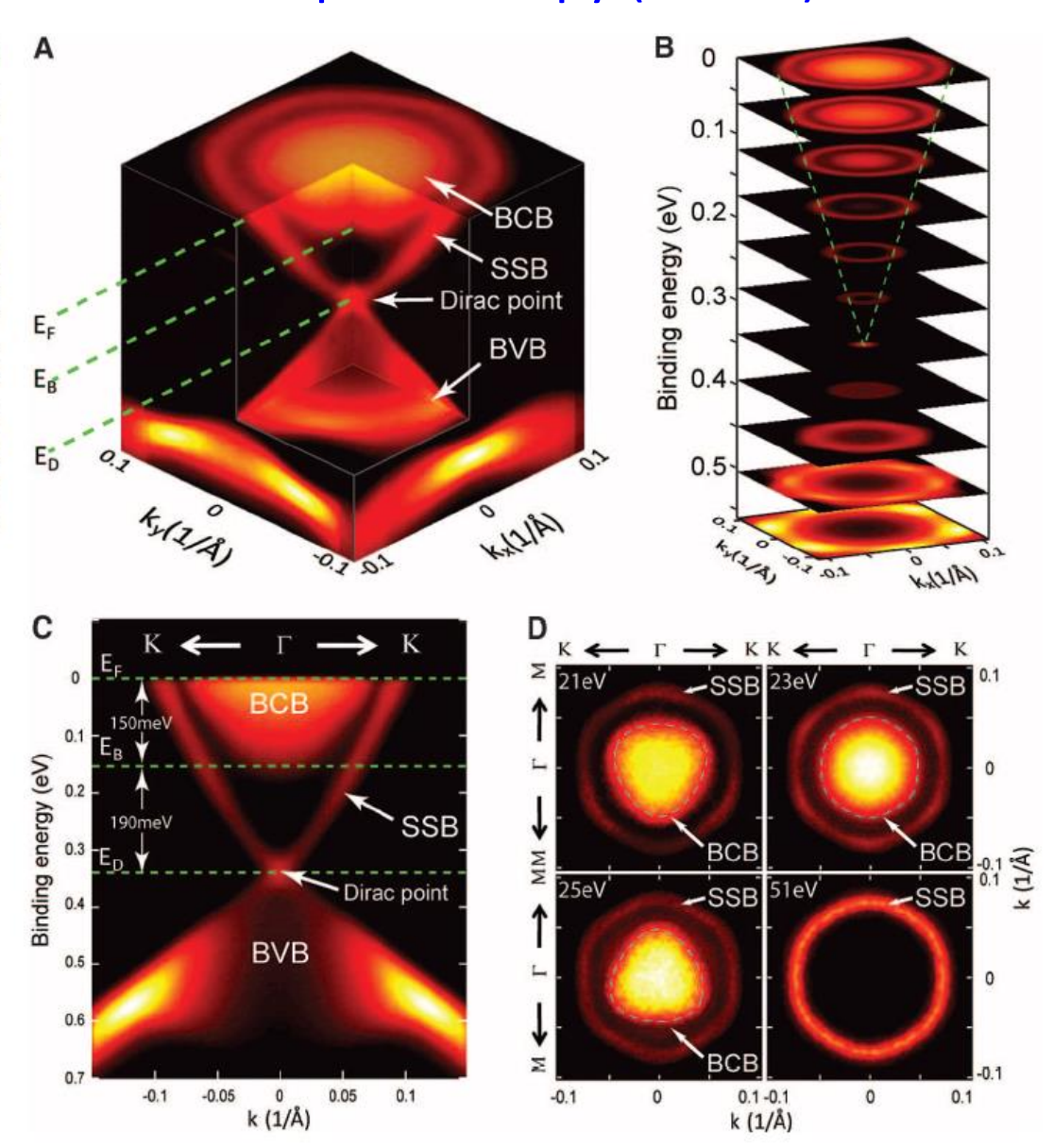
Figure 3. Mercury telluride quantum wells are two-dimensional topological insulators. (a) The behavior of a mercury telluride-cadmium telluride quantum well depends on the thickness d of the HgTe layer. Here the blue curve shows the potential-energy well experienced by electrons in the conduction band; the red curve is the barrier for holes in the valence band. Electrons and holes are trapped laterally by those potentials but are free in the other two dimensions. For quantum wells thinner than a critical thickness $d_c \simeq 6.5$ nm, the energy of the lowest-energy conduction subband, labeled E1, is higher than that of the highest-energy valence band, labeled H1. But for $d > d_c$, those electron and hole bands are inverted. (b) The energy spectra of the quantum wells. The thin quantum well has an insulating energy gap, but inside the gap in the thick quantum well are edge states, shown by red and blue lines. (c) Experimentally measured resistance of thin and thick quantum wells, plotted against the voltage applied to a gate electrode to change the chemical potential. The thin quantum well has a nearly infinite resistance within the gap, whereas the thick quantum well has a quantized resistance plateau at $R = h/2e^2$, due to the perfectly conducting edge states. Moreover, the resistance plateau is the same for samples with different widths, from 0.5 µm (red) to 1.0 µm (blue), proof that only the edges are conducting.

Angle Resolved Photo Emission Spectroscopy (ARPES)

Fig. 1. Electronic band structure of undoped Bi2Se3 measured by ARPES. (A) The bulk conduction band (BCB), bulk valence band (BVB), and surface-state band (SSB) are indicated, along with the Fermi energy $(E_{\rm F})$, the bottom of the BCB $(E_{\rm B})$, and the Dirac point (E_D) . (B) Constant-energy contours of the band structure show the SSB evolution from the Dirac point to a hexagonal shape (green dashed lines). (C) Band structure along the K- Γ -K direction, where Γ is the center of the hexagonal surface Brillouin zone (BZ), and the K and M points [see (D)] are the vertex and the midpoint of the side of the BZ, respectively (14). The BCB bottom is ~190 meV above En and 150 meV below $E_{\rm F}$. (D) Photon energy-dependent FS maps (symmetrized according to the crystal symmetry). Blue dashed lines around the BCB FS pocket indicate their different shapes.

3 D topological insulators: Bi₂Sb₃, Bi₂Se₃, Bi₂Te₃, Sb₂Te₃. There is optical proof of the Dirac cone, but no transport evidence.

M. Z. Hasan, C. L. Kane



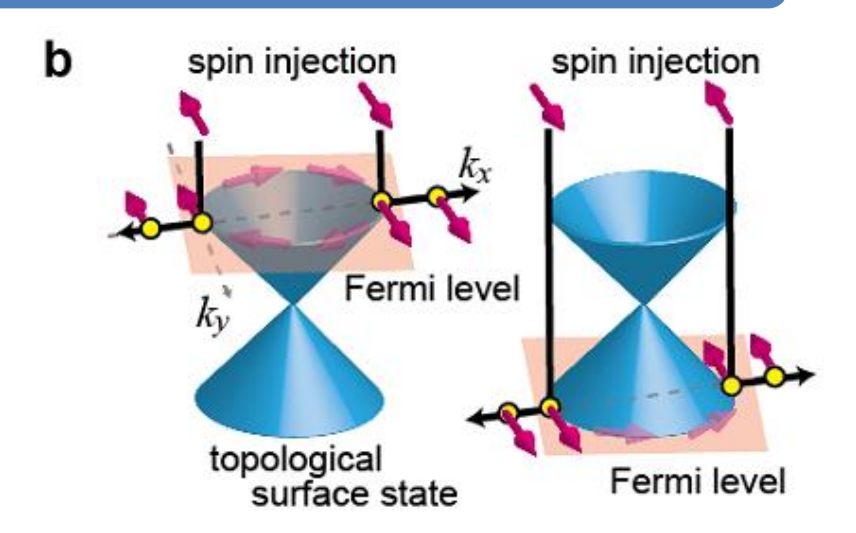
SCIENCE 329, 659 (2010)

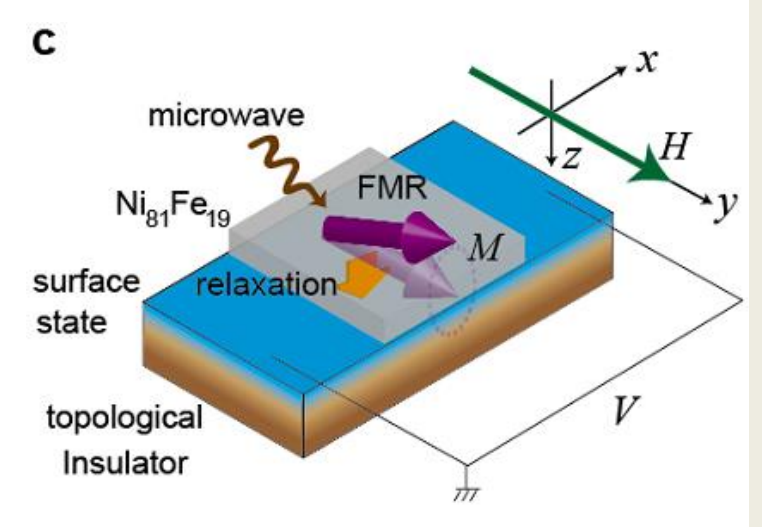
Topological insulators for Spintronic

topological insulator

topological surface state

helical
Dirac cone
bulk insulating state





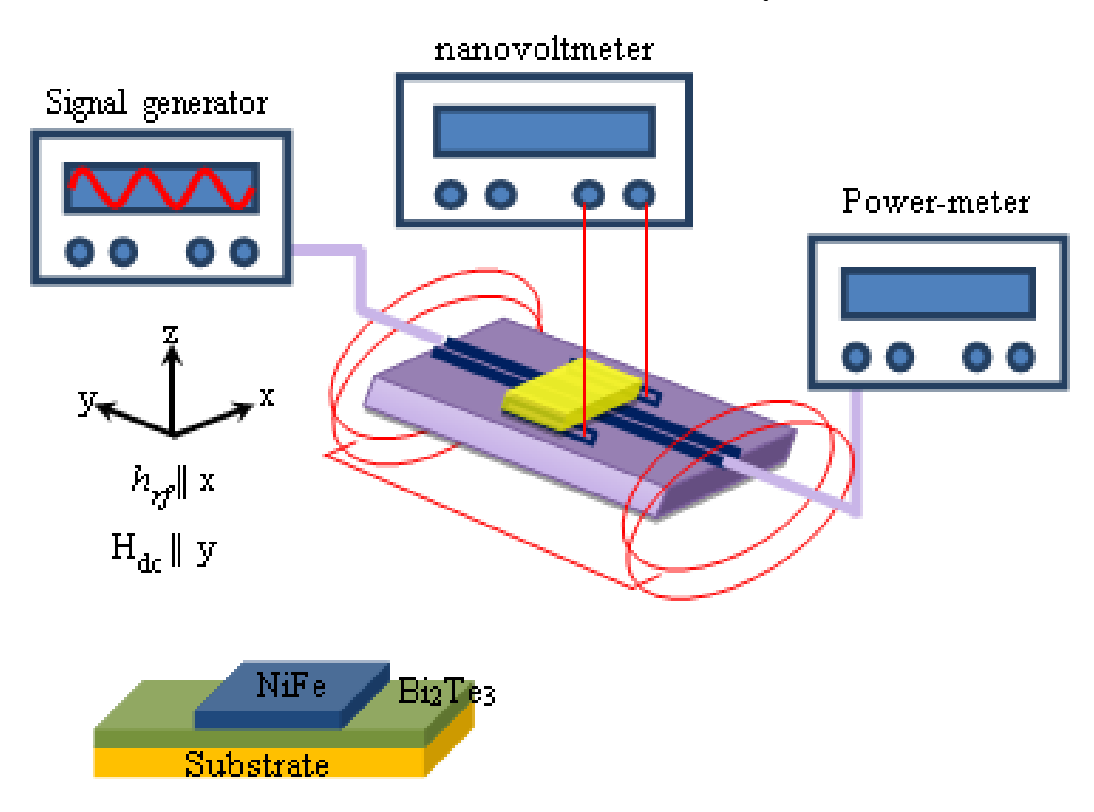
- A. TIs have topologically-protected metallic surface states.
 - Spin-momentum locking: Conduction electrons states behave as Dirac fermions.
- B. Direction of the e-motion determines its spin direction.
- C. if a spin imbalance is induced in the surface state by spin pumping, a charge current J_c is expected to show up along the "Hall" direction defined by $J_c \mid \mid \Phi(z \times \sigma)$

Shiomi et. al., arXiv1312.7091 (2013).

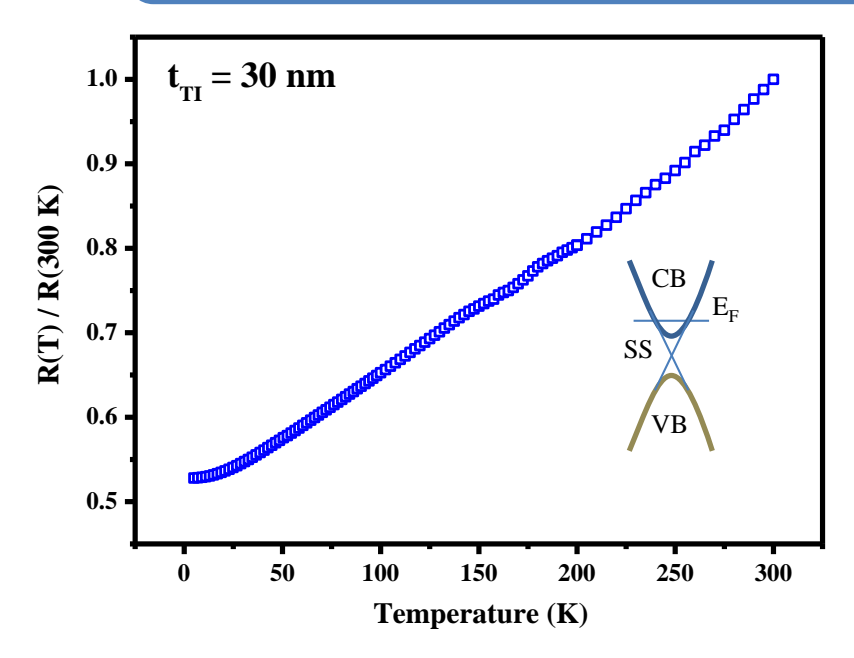
Spin Chemical Potential Bias Induced Surface Current Evidenced by Spin Pumping into Topological Insulator Bi₂Te₃

Faris Basheer Abdulahad, Jin-Han Lin, Yung Liou, Wen-Kai Chiu, Liang-Juan Chang, Ming-Yi Kao, Jun-Zhi Liang, Dung-Shing Hung, and Shang-Fan Lee

PRB Rapid Comm. **92**, 241304R (2015)

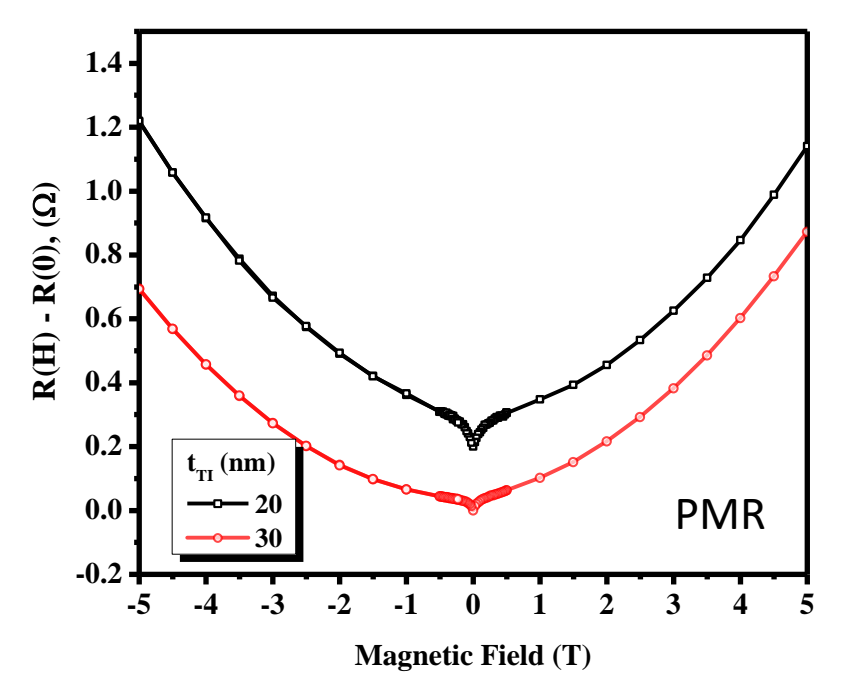


Transport measurements on Bi₂Te₃ films grown on sapphire (0001)

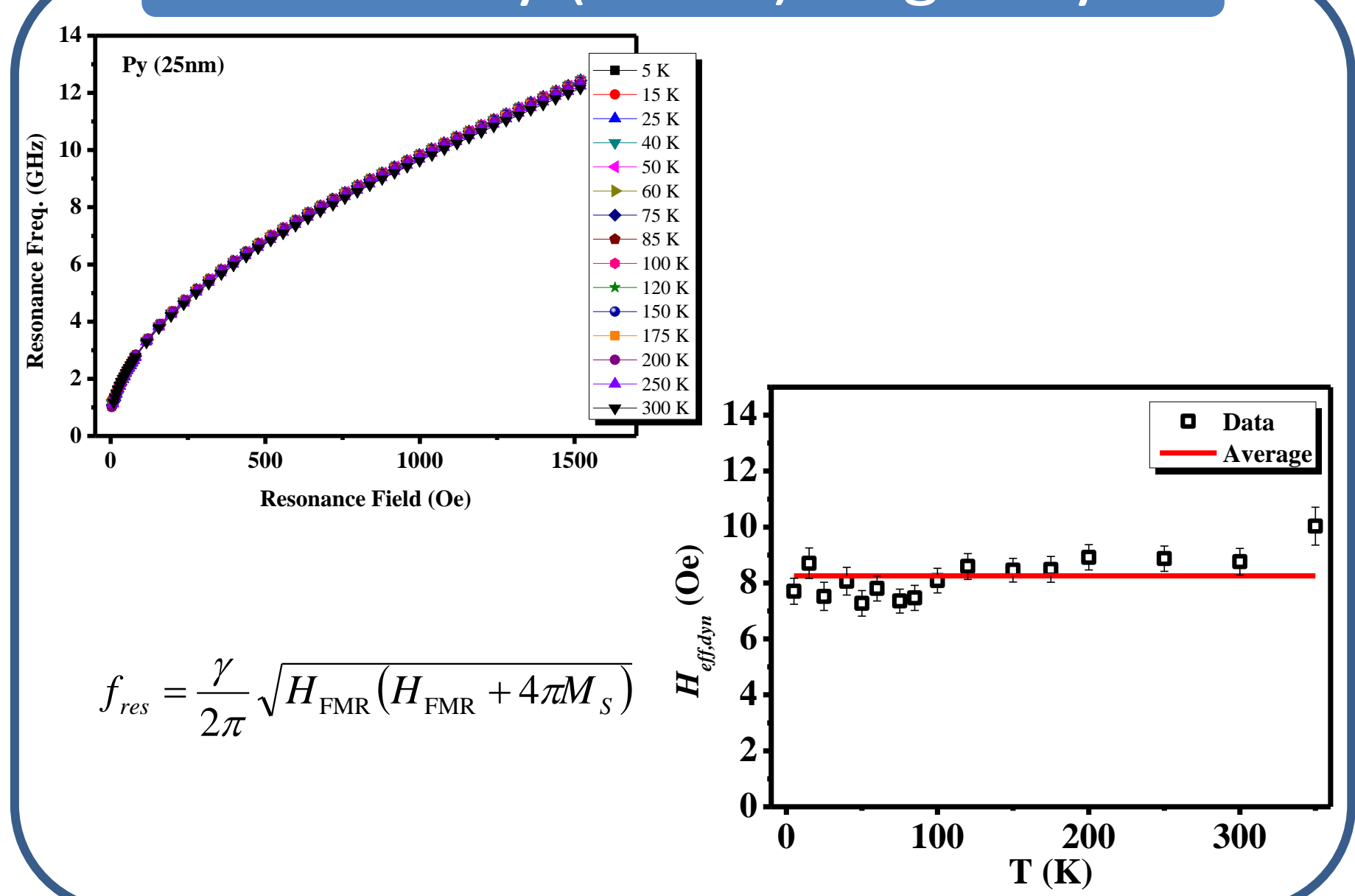


Temperature dependence of normalized resistivity for 30 nm sample measured under zero magnetic field. Inset shows the schematic illustration of the Fermi level.

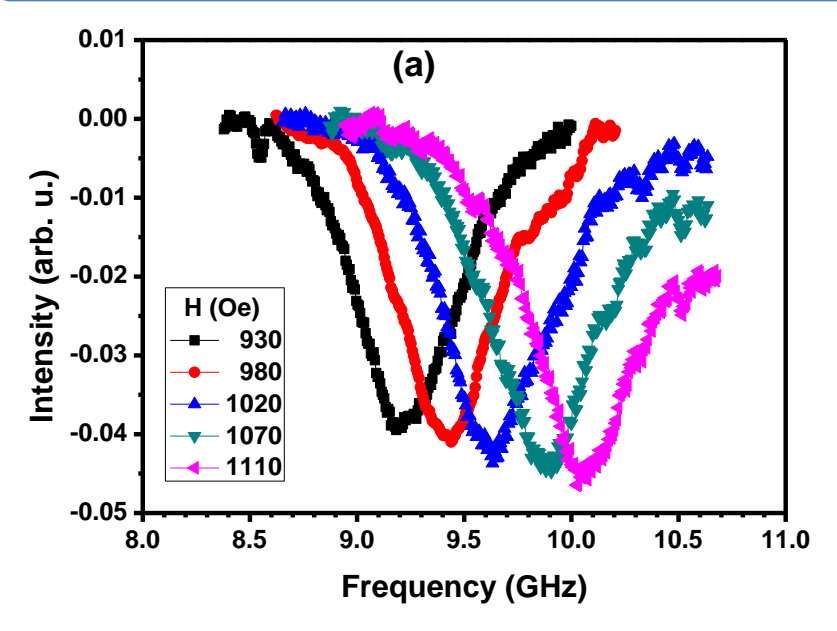
Magnetic field dependence of normalized resistivity for 20 nm (black) and 30 nm (red) samples at T = 5 K. The black curve is shifted for clarity.



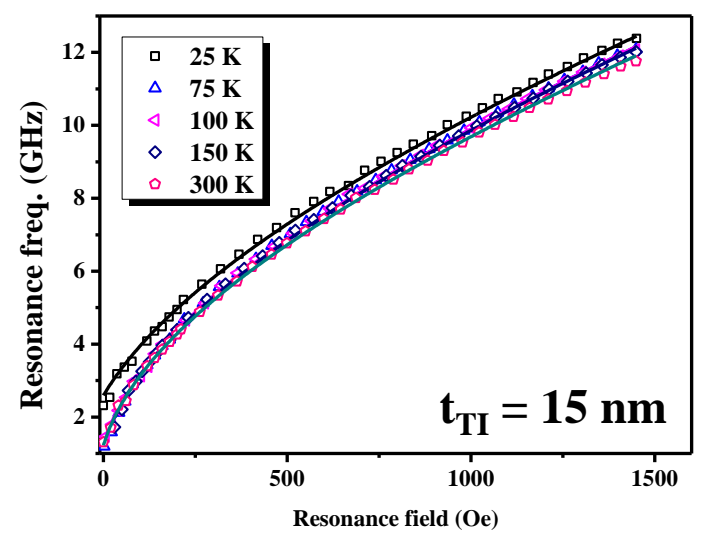
FMR for Py (25nm) single layer

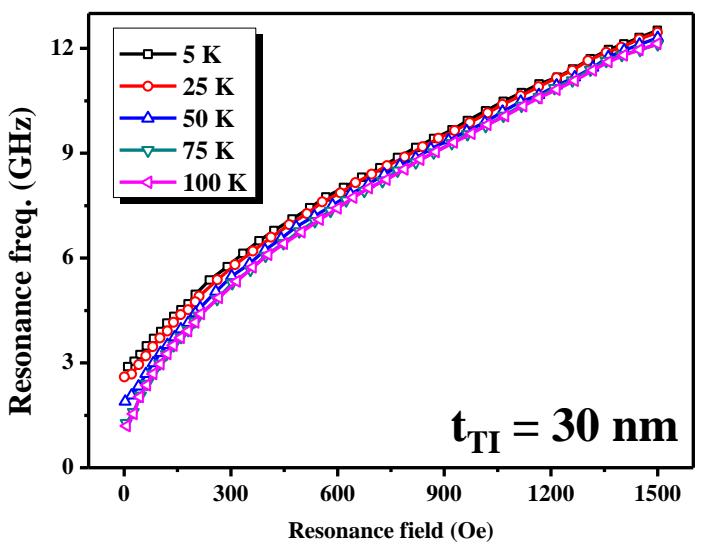


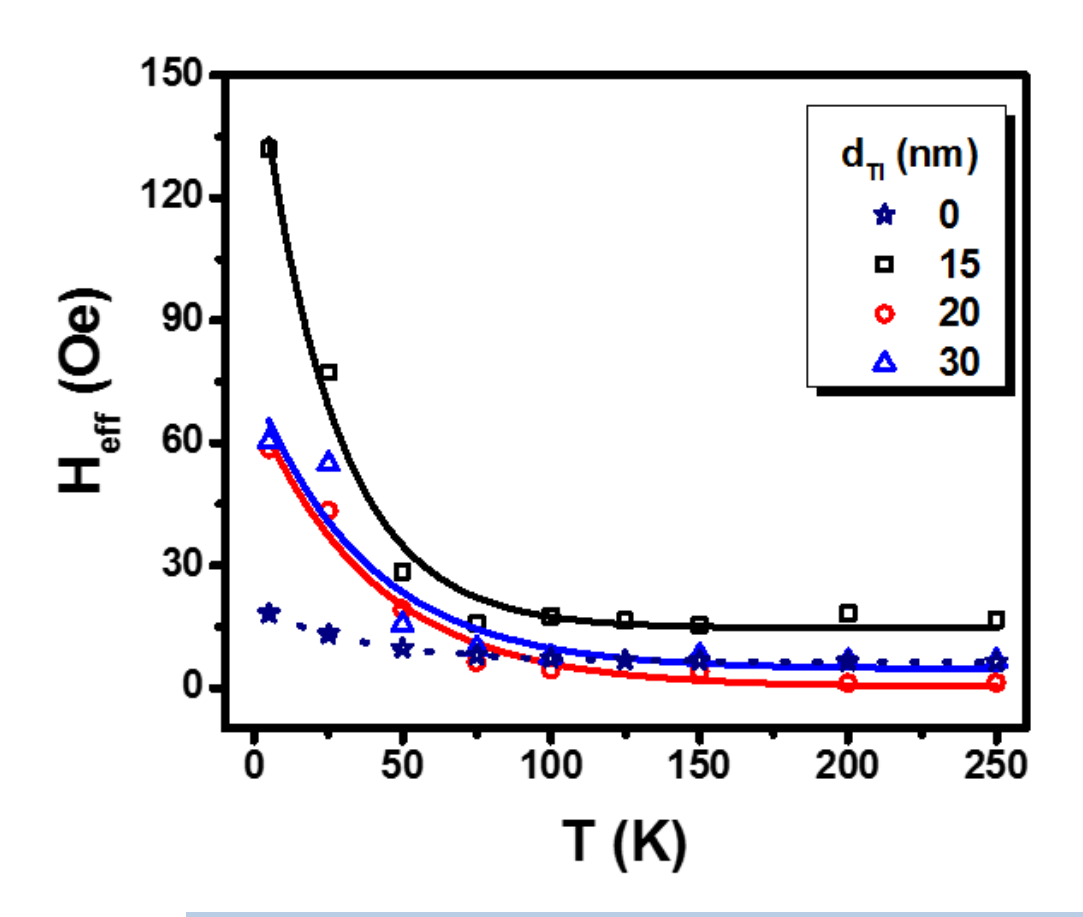
FMR for Bi₂Te₃/Py Bilayers



Temperature dependence measurements of FMR show upper left shift compared to single Py layers.







Possible effects:

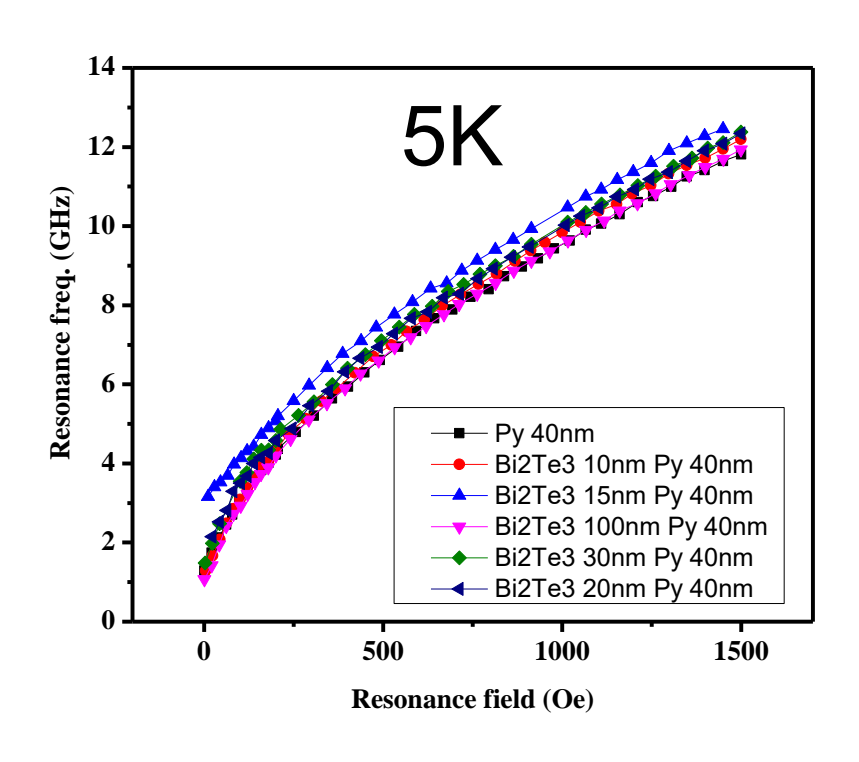
- FM-anisotropy
- Proximity effect
- FM/TI exchange coupling.

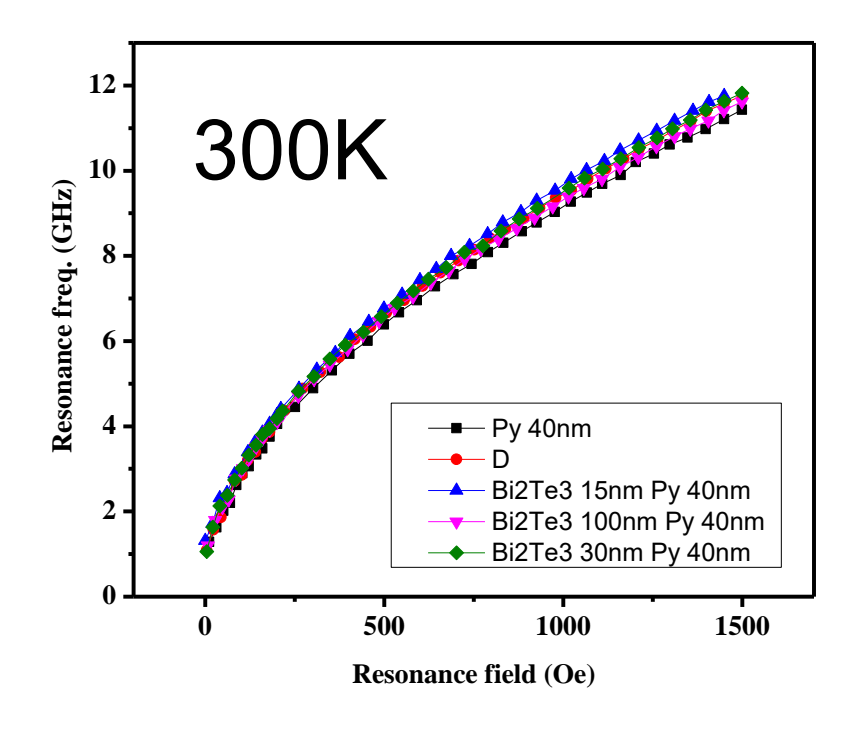
$$f_{res} = \frac{\gamma}{2\pi} \sqrt{(\mathbf{H}_0 + \boldsymbol{H}_{eff})((\mathbf{H}_0 + \boldsymbol{H}_{eff}) + 4\pi \boldsymbol{M}_S)}$$

Temperature dependence of the effective field for the reference sample and 15, 20, and 30 nm Bi₂Te₃ samples. Solid lines are exponential fits.

Bi₂Te₃/Py Bilayers

Bi₂Te₃ thickness dependence of FMR





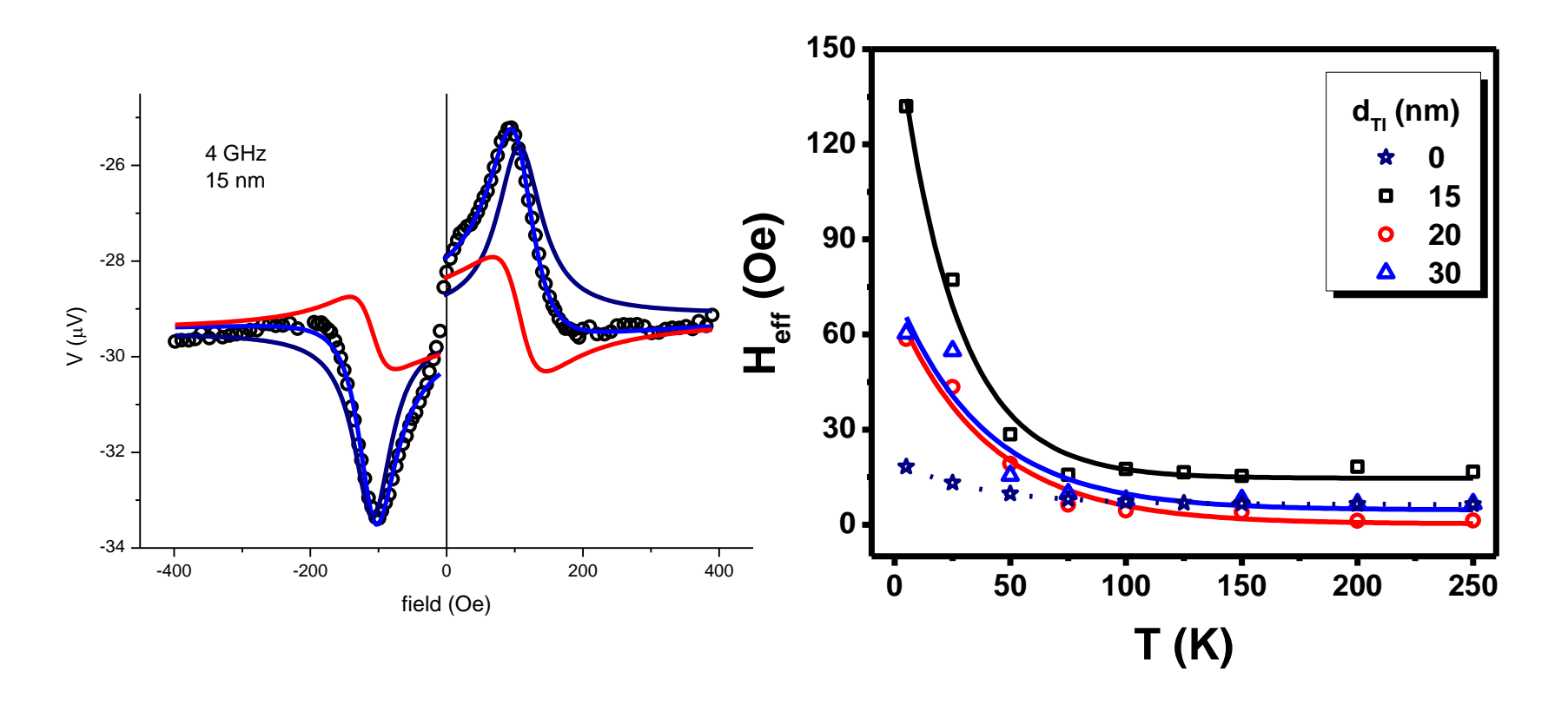
Bi₂Te₃/Py Bilayers

H_{eff} for Bi₂Te₃ thickness dependence

	Υ =1.8887E7 ; M_s =8863.2 Oe (5K) Υ =1.88264E7 ; M_s =8271.3 Oe (300K)	
	5K	300K
Py (40nm)	18.26 <u>+</u> 1 Oe	6.64 <u>+</u> 1 Oe
Bi ₂ Te ₃ (10nm)/ Py (40nm)	27.79 <u>+</u> 3.6 Oe	22.16 <u>+</u> 3.43 Oe
Bi ₂ Te ₃ (15nm)/ Py (40nm)	132 <u>+</u> 5.5Oe	44 <u>+</u> 5.4Oe
Bi ₂ Te ₃ (20nm)/ Py (40nm)	58.5 <u>+</u> 4.25Oe	_
Bi ₂ Te ₃ (30nm)/ Py (40nm)	60.344 <u>+</u> 5.5Oe	29 <u>+</u> 3.70e
Bi ₂ Te ₃ (100nm)/ Py (40nm)	12.17 <u>+</u> 1.1 Oe	19.8 <u>+</u> 1.9 Oe

Summary

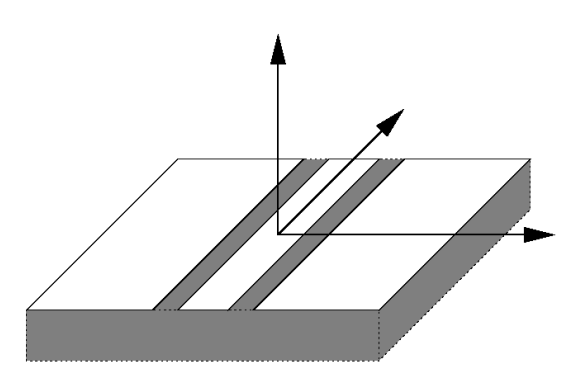
- 1. Large H_{eff} due to the spin pumping effect was observed for different Bi₂Te₃ thin films.
- 2. H_{eff} has a maximum value around $t_{TI} = 15$ nm.
- 3. H_{eff} increases with decreasing temperature; characteristic temperature $T_0 \sim 25-33$ K is on the energy scale of 2.5 meV.



We observed an exchange coupling between NiFe and TI surface. The strength of this coupling decay with increasing temperature with a characteristic temperature ~25K, or ~2.2 meV.

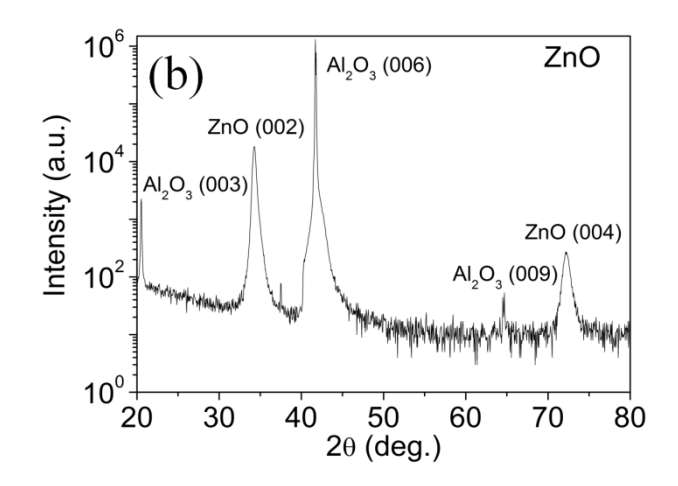
Our results on Spin Pumping in ZnO/Py film

co-planar waveguide



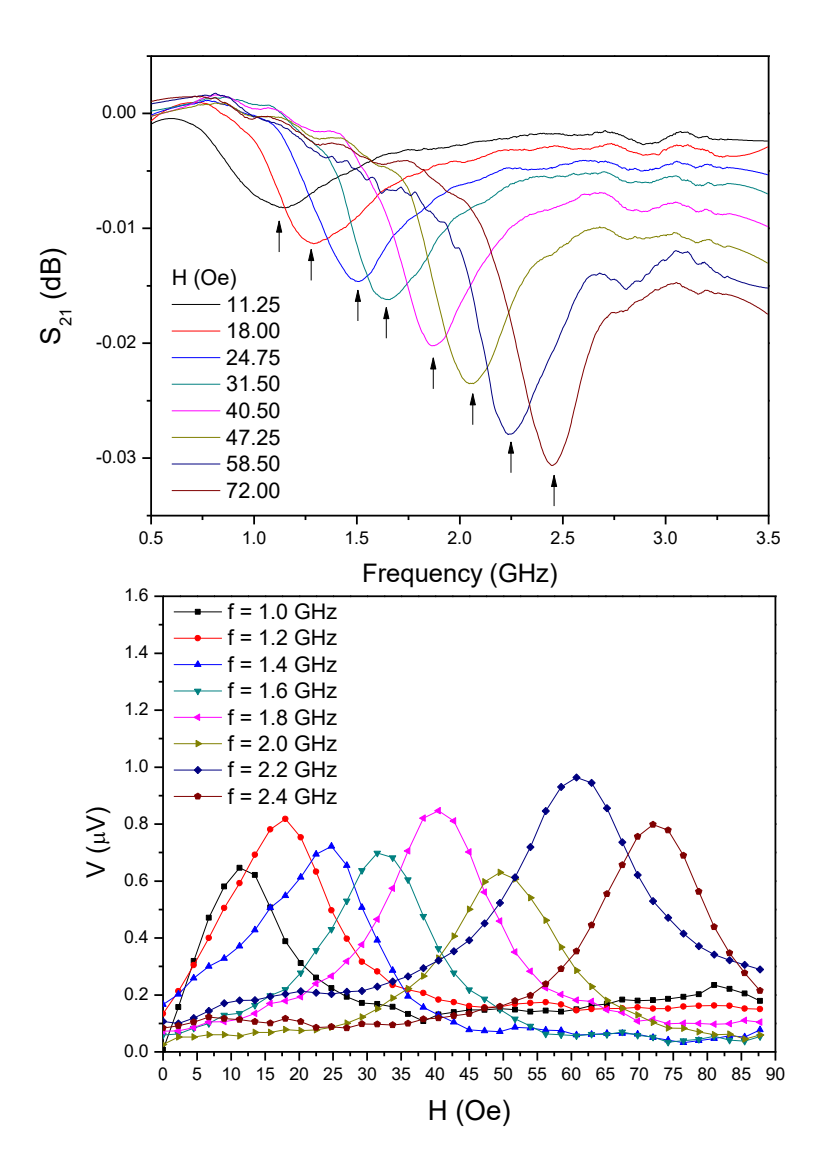
(a) 2.5mm Y H A mm

ZnO: Resistivity 0.014 Ω -cm carrier concentration 6.09 \times 10¹⁸ cm⁻³ mobility 72.9 cm²/V-s

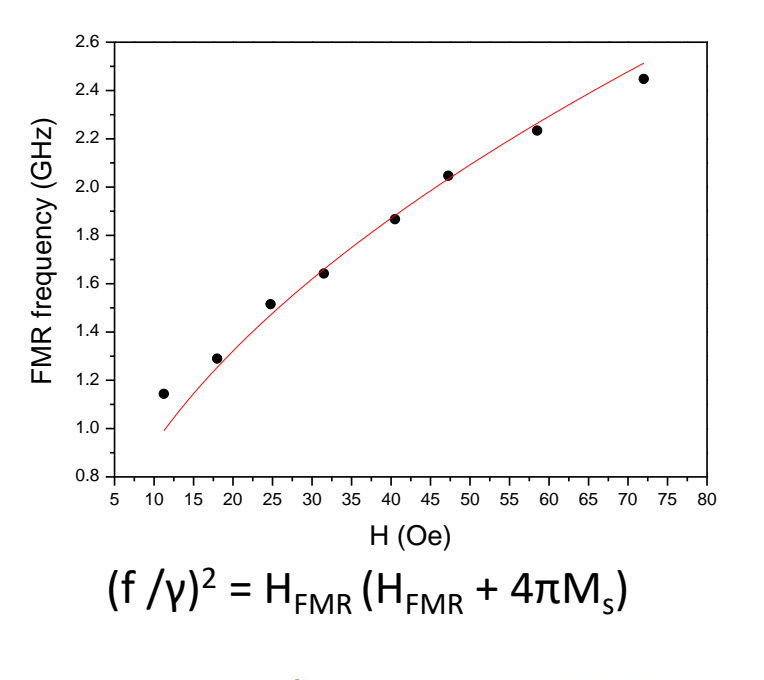


"Inverse spin Hall effect induced by spin pumping into semiconducting ZnO", APL **104**, 052401 (2014)

The FMR spectra of ZnO/Py samples



Magnetic field H dependence of electromotive force V measured for the $Ni_{80}Fe_{20}/ZnO$ thin film under 50 mW microwave excitation.



$$V = L \frac{\Delta H^2}{(H - H_0)^2 + \Delta H^2} + D \frac{\Delta H(H - H_0)}{(H - H_0)^2 + \Delta H^2},$$

Lorentz and dispersive line shapes

$$\mathbf{E}_{\mathrm{ISHE}} \propto \mathbf{J}_{s} imes oldsymbol{\sigma}$$

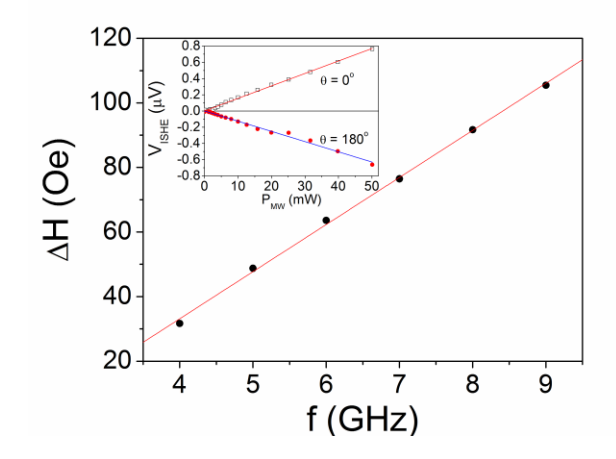
$$V_{ISHE} = \frac{W_F \theta_{SH} \lambda_N \tanh(\frac{d_N}{2\lambda_N})}{d_N \sigma_N + d_F \sigma_E} (\frac{2e}{\hbar}) j_s^0$$

$$j_{s}^{0} = \frac{g_{r}^{\uparrow\downarrow} \gamma^{2} h_{rf}^{2} \hbar [4\pi M_{s} \gamma + \sqrt{(4\pi M_{s})^{2} \gamma^{2} + 4\omega^{2}}]}{8\pi \alpha^{2} [(4\pi M_{s})^{2} \gamma^{2} + 4\omega^{2}]}$$

Considering spin back flow,

$$E_{y} = \frac{2e/\hbar}{\sigma_{N}d_{N} + \sigma_{F}d_{F}} [j_{1s}^{z}(0)\theta_{SH}^{N}\lambda_{sd}^{N} \tanh \frac{d_{N}}{2\lambda_{sd}^{N}} + j_{2s}^{z}(0)\theta_{SH}^{F}\lambda_{sd}^{F} \tanh \frac{d_{F}}{2\lambda_{sd}^{N}}]$$

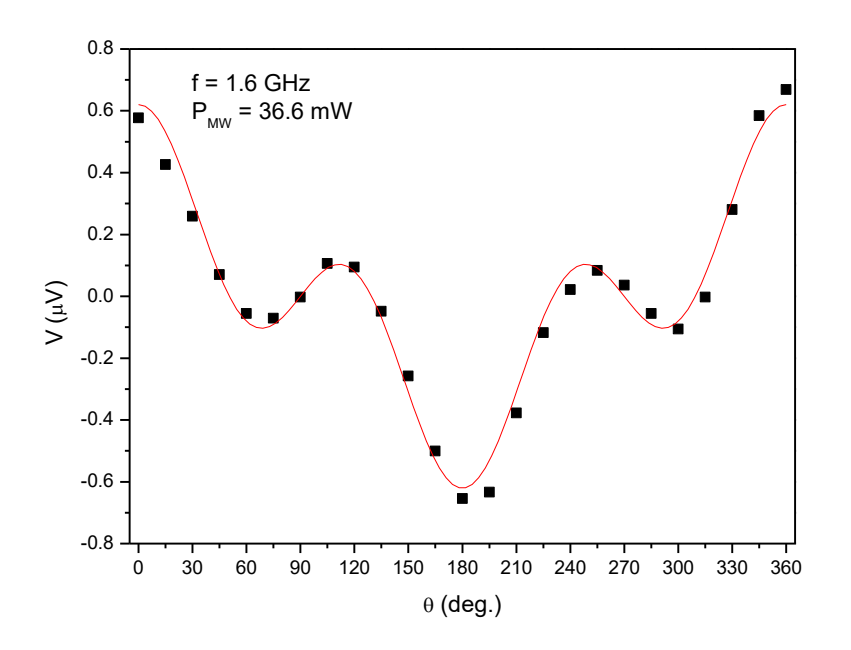
Spin mixing conductance $g_r^{\uparrow\downarrow}$ is the essential parameter to the spin pumping experiment. It refers to the efficiency of generating a spin current



$$\alpha = \frac{g\mu_B}{4\pi M_c d_E} g_r^{\uparrow\downarrow}$$

$$\Delta H_{FMR} = \Delta H_0 + \frac{2\alpha}{\gamma} f$$

$V_{dc}(H,\theta) = V_{AMR}[L(H)\cos\phi + L'(H)\sin\phi]\sin(2\theta)\sin\theta + V_{ISHE}L(H)\cos\theta$



$$L(H) = \frac{\Delta H^2}{(H - H_{FMR})^2 + \Delta H^2}$$

$$L'(H) = \frac{\Delta H(H - H_{FMR})}{(H - H_{FMR})^2 + \Delta H^2}$$

The in-plane angle θ dependence of the electromotive force V or Ni₈₀Fe₂₀ / ZnO thin film. The solid symbols are the experimental data and the red line is the theoretical fitting line.

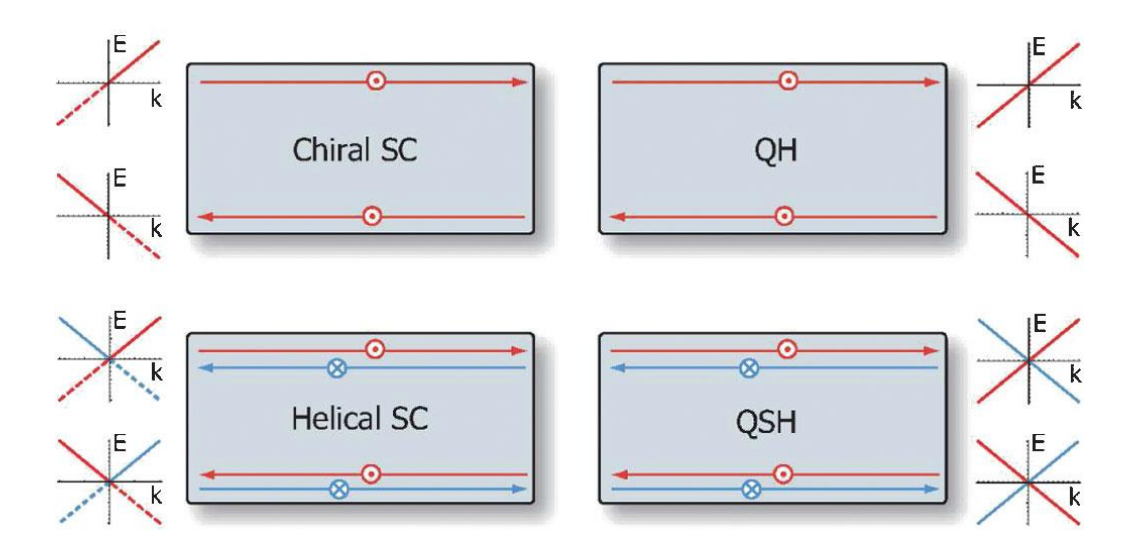
Magnonic charge pumping? PRB **92**, 024402 (2015)

PHYSICAL REVIEW B 83, 144402 (2011)

Spin pumping and anisotropic magnetoresistance voltages in magnetic bilayers: Theory and experiment

A. Azevedo, ^{1,*} L. H. Vilela-Leão, ¹ R. L. Rodríguez-Suárez, ² A. F. Lacerda Santos, ¹ and S. M. Rezende ¹ Departamento de Física, Universidade Federal de Pernambuco, Recife, Pernambuco 50670-901, Brazil ² Facultad de Física, Pontificia Universidad Católica de Chile, Casilla 306, Santiago, Chile (Received 6 June 2010; revised manuscript received 29 January 2011; published 4 April 2011)

Topological insulators and topological superconductors



Schematic comparison of 2D chiral superconductor and QH states. In both systems, TR symmetry is broken and the edge states carry a definite chirality. (Bottom row) Schematic comparison of 2D TR invariant topological superconductor and QSH insulator. Both systems preserve TR symmetry and have a helical pair of edge states, where opposite spin states counterpropagate. The dashed lines show that the edge states of the superconductors are Majorana fermions so that the E<0 part of the quasiparticle spectrum is redundant. In terms of the edge state degrees of freedom, we have symbolically QSH = $(QH)^2 = (helical SC)^2 = (chiral SC)^4$.

From Qi, Hughes et al., 2009a.

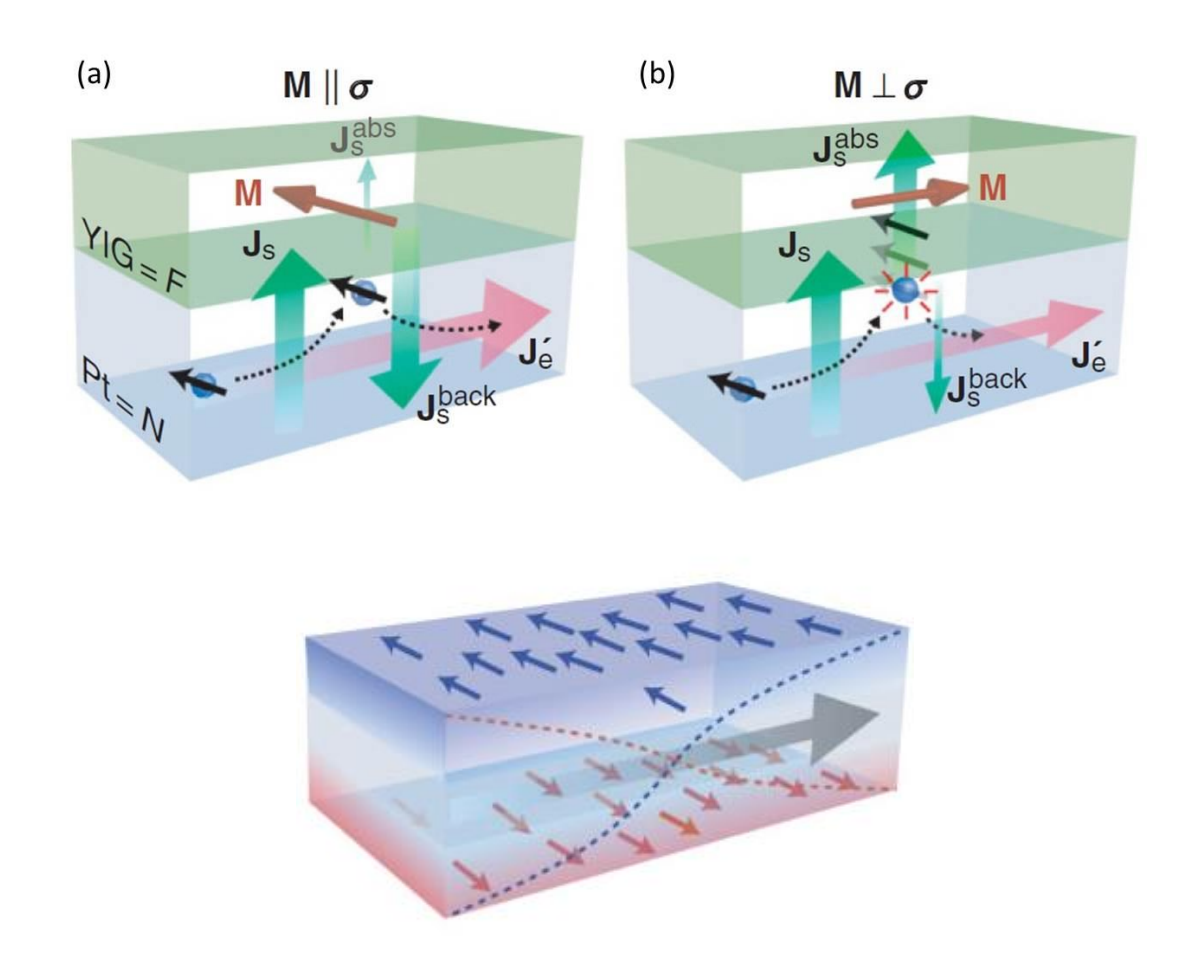
REVIEWS OF MODERN PHYSICS, 83, 1057 (2011) DOI: 10.1103/RevModPhys.83.1057

Summary

- Giant Magnetoresistance, Tunneling Magnetoresistance
- Spin Transfer Torque
- Pure Spin current (no net charge current)
 - Spin Hall, Inverse Spin Hall effects
 - Spin Pumping effect
 - Spin Seebeck effect
- Micro and nano Magnetics
- Spin pumping into Topological Insulator, Topological Superconductor
- Spin logic
- Skyrmion

Q: Is "spintronics" the next generation technology beyond 2020?
There is no better candidate in sight ?!

Spin Hall Magnetoresistance



PRL **110**, 206601 (2013)

Spin Hall Magnetoresistance Induced by a Nonequilibrium Proximity Effect

Spintronics has evolved in many aspects other than material developments, including effects like Giant Magnetoresistance, Tunneling Magnetoresistance, Spin Transfer Torque, Spin Hall, Spin Pumping, Inverse Spin Hall, and more. The underlying idea was to investigate and manipulate the electron spin degree of freedom in addition to its charge in transport phenomena. However, charge transport is usually accompanied by Joule heating problem as the sizes of the electronics continue to shrink. Thus, devices that manipulate pure spin currents can be highly beneficial compared to traditional charge-based electronics. We now have "spin caloritronics", where one exploits the interaction between heat transport and the charge/spin carriers.

Spin caloritronic effect, such as spin Seebeck effect, has attracted a great deal of attention recently. The difference in the chemical potentials of the spin-up and the spin-down electrons can cause a pure spin current. This pure spin current can be detected by Pt strips via the inverse spin-Hall effect. In most cases such studies have been made on ferromagnetic thin films on substrates. The mechanism of spin Seebeck effect has evolved from the above-mentioned intrinsic difference in the spin chemical potentials when it was first reported experimentally to magnon-phonon interaction through the substrate in recent publication. We use patterned ferromagnetic thin film to demonstrate the profound effect of a substrate on the spin-dependent thermal transport [1]. With different sample patterns and on varying the direction of temperature gradient, both longitudinal and transverse thermal voltages exhibit asymmetric instead of symmetric spin dependence. This unexpected behavior is due to an out-of-plane temperature gradient imposed by the thermal conduction through the substrate and the mixture of the anomalous Nernst effects. Only with substrate-free samples have we determined the intrinsic spindependent thermal transport with characteristics and field sensitivity similar to those of anisotropic magnetoresistance effect.